

5.2 SWIFT HEAVY IONS IN MATERIALS

D.K. Avasthi and D. Kanjilal

There has been a large variety of experiments on modification of materials, surface and interfaces by high energy heavy ion beams. A summary of these experiments is given here.

The effect of swift heavy ions at the interfaces of W/C, V/Si, Co/Ge, Cu/Ge, Au/Ge, and Si/C₆₀ have been investigated by different groups. Hypothesis of the interdiffusion at the interface during transient melt phase as a cause of SHI induced mixing, suggested in previous years by the group at NSC is getting further support. The mixing in Si/fullerene and V/Si systems is explained on this basis. One must add here that there are effects of nuclear energy loss contributing to the mixing. There have been two approaches to consider this. The first one considers it as additive effect but insignificant (less than 10 percent) based on the extrapolation of the results on the mixing induced by nuclear energy loss. The second one considers that the effect of nuclear energy loss enhances the effect electronic energy loss significantly. However detailed calculations will be required to settle this issue. Some work in Fe/Si system is in progress currently, which will answer this questions hopefully in the report of next year. High resolution microscopy has been performed to investigate the the Au-Ge alloy formed at the Au/Ge interface as a result of irradiation. The findings in W/C experiment of SHI induced mixing that the mixing efficiency is higher for thinner film is well explainable by thermal spike model.

The experiments on the SHI irradiation of GaN shows that the band gap can be engineered (from 3.4 eV to 3.0 eV) by the irradiation fluence. The resistivity of ZnO thin film is shown to be decreasing with fluence and is attributed to the vacancies of oxygen created by the ion irradiation. The fullerene film irradiation shows the signature of the formation of dimers and the band gap is found to be reducing with the fluence.

Luminescence studies of the Si nano particles formed by keV and MeV ion beam have been performed.

SHI irradiation effects on various type of ferrite films have been studied. It is shown that the magnetization increases at a low fluence of 10^{11} ions/cm² and then it decreases with further increase in fluence. The increase in the magnetization is shown to be due to the texturing of the films, evident by the XRD.

The grain size in the LiF thin films decreases and the F₂ as well as F₃ centers increase with the fluence. The PI in mullite samples decreases with fluence. The changes in chemical bonds in irradiated polyanilin films are studied by FTIR. Thermally simulated polarizing and thermally simulated depolarizing studies are performed in irradiated Kapton films. Gas permeation studies in asymmetric membrane formed by the chemical

etching of the irradiated polymers have been performed. Free volume studies in SHI irradiated PET are performed. The successful use of OHP foils is demonstrated for the use as nuclear track detector. Straggling and energy loss measurements are performed in several polymers for different ions and energies.

Single event studies are performed in EEPROM, shift register, bus controller etc. for simulating the cosmic radiation effects on electronic components in space.

Correlation of the track diameters with the charge state of the incident ions is investigated by the study of H loss behavior in polymers. H loss was found to be dependent on the charge state of the incident ion. A test run of 12 MeV C RBS was performed successfully, giving a depth resolution of about 10 nm.

5.2.1 Study of thickness effect on intermixing in W/C multilayer with Swift heavy Ion irradiation

Amit Saraiya¹, Satish Potdar¹, D. K. Avasthi² and Ajay Gupta¹

¹Inter-University Consortium for DAE Facilities, University Campus, Khandwa Road, Indore-452 017

² Nuclear Science Centre, New Delhi-110067

Swift heavy-ion-induced modifications in thin films and multilayer has attracted attention in recent years. Swift heavy ions can induce significant modifications in metallic systems above a threshold value of the electronic energy loss (S_e), which varies considerably from metal to metal. In the present work, effect of the thickness of individual layer on the efficiency of intermixing in W/C multilayer has been studied. The observed results support the thermal spike model^{1,2} for SHI induced intermixing in multilayer.

Two different sets of multilayer (set-A) Float glass/[W (14.2 Å)/ C (21.3 Å)]x10 and (set -B) Float glass/[W (5.9 Å)/ C (8.8 Å)]x10 were deposited by ion beam sputtering. In both the samples W and C thickness were kept in ratio 2:3. Kaufman type hot cathode ion source (3.0 cm Commonwealth Scientific Corporation) was used to alternately sputter high purity W and C targets. A base pressure of 2×10^{-7} Torr was achieved before deposition using oil free vacuum pump and the samples were deposited in 1.7×10^{-4} Torr base pressure. Deposited samples were irradiated with 120 MeV Ag^+ ion to a fluence of 5×10^{13} ions /cm² using 15UD Pelletron at Nuclear Science Center, New Delhi. The samples were characterized with X-ray reflectivity using D5000 Diffractometer with Cu $K\alpha$ radiation source. XRR data was fitted with Parratt formalism.³

Simulation using TRIM code suggest that electronic and nuclear energy loss values for the Carbon are 14.3 keV /nm, 0.05keV/nm and for tungsten 36keV/nm, 0.24keV/nm respectively with Ag ion of 120 MeV. The nuclear energy loss in both C and W is negligible compare to electronic energy loss, therefore modifications in multilayer

are expected to occur mainly due to electron energy loss. Fig.1 a and b shows the XRR pattern of set-A before and after irradiating with 120 MeV Ag ion. The solid line represents the best fit to the data, the corresponding electron density profiles are given in Fig. 1- c and d, one may note that irradiation results in only a small intermixing (about 1 Å) at each interface. Fig. 2-a to d shows the corresponding results of set-B. Fig. 2-c and d shows that in this sample irradiation results in a complete intermixing of W and C layer. These results show that there is a significant difference in the intermixing in the two specimens although the electron energy loss per unit length is same in both the samples. A higher mixing efficiency in the multilayer of set-B, having smaller individual layer thickness may be understood in terms of thermal spike model.

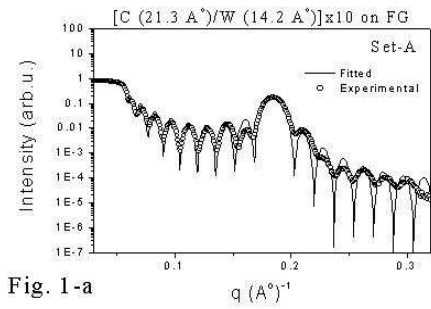


Fig. 1-a

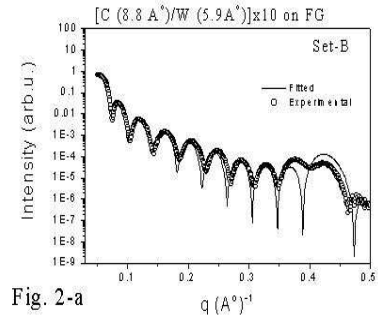


Fig. 2-a

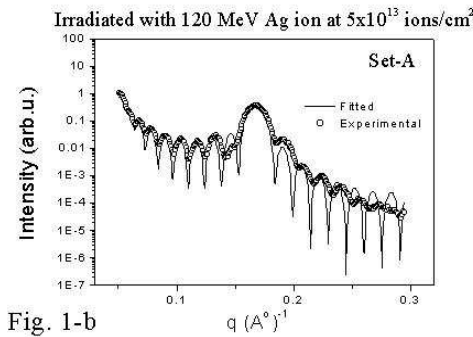


Fig. 1-b

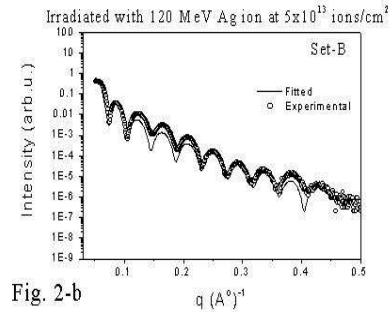


Fig. 2-b

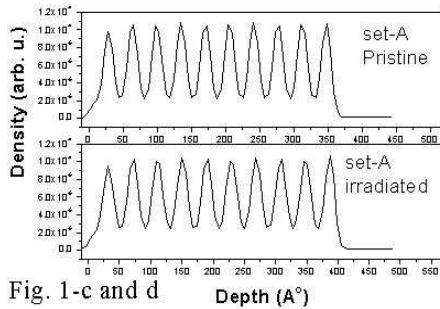


Fig. 1-c and d

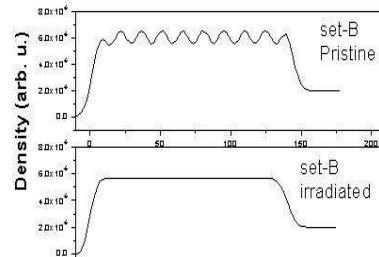


Fig. 1: XRR patterns of set-A with the fitting a) pristine b) irradiated ; electron density profile of the same c) pristine d) irradiated.

Fig 2: XRR patterns of set-B with the fitting a) pristine b) irradiated ; electron density profile of the same c) pristine d) irradiated

Swift heavy-ion deposits a large amount of energy in the electronic system of the target. Electron-electron interaction redistributes the energy within the electronic system leading to the thermalisation of the energy. This occurs at a time scale of 10^{-15} to 10^{-14} s. Electron-lattice interaction causes energy to transfer from electron system to lattice and thus inducing a lattice temperature increase at a time scale of 10^{-13} – 10^{-12} s. Temperature of the thermal spike thus generated depends upon, the volume in which the energy imparted by the SHI diffuses due to the mobility of the δ -electron. Scattering of the δ -electrons from the thin film surfaces, interfaces, and also from the grain boundaries will reduce the mobility of the δ -electron as well as will increase the electron-phonon interaction. In set-B, because of a larger number of interfaces per unit length, the electron scattering will be stronger, which will result in the reduced mobility of δ -electron. The energy deposited by the bombarding ion in the electronic system will remain confined to a smaller volume around the ion track. This in turn will result in a higher temperature in the thermal spike region⁴, causing mixing efficiency to increase. It may be noted that with decreasing layer thickness the interface energy per unit volume increases, which would act as an additional thermodynamic driving force for intermixing. This would also cause the mixing efficiency to increase.

REFERENCES

- [1] Z.G. Wang, Ch Dufour, E. Paumier, M. Toulemonde, J.Phys. Condens Matter 6 (1994) 6733.
- [2] Ajay Gupta, Vacuum 58 (2000) 16.
- [3] L. G. Parratt, Phys. Rev. 95 (1954) 359.
- [4] Ajay Gupta and D. K. Avasthi, Physical Review B, 64 (2001) 155407.

5.2.2 Investigation of V/Si mixing induced by Swift Heavy Ions

K. Diva¹, D. Kabiraj², B.R. Chakraborty¹, S.M. Shivaprasad¹ and D.K. Avasthi²

¹Surface Physics Group, National Physical Laboratory, New Delhi –110012

²Nuclear Science Centre, New Delhi - 110067

Ion beam mixing [IBM] has been of interest for the synthesis of silicides in various compound phases. This is a phenomenon of atomic migration across an interface under the influence of energetic ions. IBM has definite advantages over the conventional methods of synthesis in terms of spatial selectivity, precise control and relatively low temperature process. IBM with lower energy ion has been well studied and a good understanding exists about the basic mechanism as being due to nuclear energy loss [1]. There-

fore it was expected that IBM process will reduce at higher energies where the nuclear energy loss decreases and becomes insignificant. However it has been observed in the early 90's that high energy heavy ions can also induce mixing at the interface of metal/ Si system [2, 3]. Qualitatively, the atomic migration across the interface, due to the electronic energy loss of high energy heavy ions, were explained by the thermal spike model [4]. First quantitative explanation in the framework of thermal spike model was given for the transport of oxygen atoms across the interface [5]. It was suggested that the diffusion of oxygen across the interface in CuO/float glass system occurred during the transient melt phase. Duration of the molten phase and the radius of the ion track were taken from the existing theoretical prediction and the spatial spread of oxygen at the interface enabled the determination of the diffusion coefficient of oxygen as $\sim 10^{-6}\text{m}^2\text{s}^{-1}$. Such a high diffusivity is possible only in liquids and thus the existence of a transient molten phase was proved to be the cause of atomic transport across the interface. Wang et al [5] suggested several metals to be sensitive to electronic energy loss (S_e) beyond certain threshold. SHI induced mixing in the metal/Si and metal/metal systems known so far (e.g. Fe/Si, Ti/Si, Ni/Ti), has such metals which are known to be sensitive to S_e . In the present case, we have chosen the metal V on Si, where the information about the sensitivity of V on electronic excitation is not known. Therefore the mixing in V/Si, if observed with 120 MeV Au ions will indicate the sensitivity of V to electronic excitation. The ion and energy is chosen in such a way that it provides the maximum possible S_e from the Pelletron accelerator at NSC.

The Si/V/Si samples (prepared in oil free clean vacuum of 10^{-8} mbar) were irradiated by 120 MeV Au ions using 15 UD Pelletron at NSC Delhi, for fluences in the range of 1×10^{13} to 1×10^{14} ions/cm² at room temperature. The samples were irradiated uniformly over an area of 1cm x 1cm by scanning the ion beam with a current <1 particle nano Ampere (pA) using an electromagnetic scanner. The energy loss values are estimated using simulation program SRIM, according to which the values of electronic energy loss of 120 MeV Au in Si and V are 1.4 keV/Å and 2.9 keV/Å. The corresponding nuclear energy loss values are 2.1×10^{-2} keV/Å and 4.5×10^{-2} keV/Å respectively indicating that the energy loss process by electronic excitation is dominant. Therefore the observed mixing at the interface can be envisaged to be due to the electronic energy loss deposition. Although the influence of nuclear energy loss does exist in the present case, it is considered to be insignificant (<10%).

Since the present case involves V, a metal, the possibility of Coulomb explosion is ruled out because of the high mobility of conduction electrons. The other possibility is the thermal spike model, which has already been successfully employed even in several insulator/insulator system to show that interface mixing is due to inter diffusion in the melt phase. The present V/Si mixing is a better case to consider under the formalism of the thermal spike model. An approximate estimate of the diffusivity in the molten state is made for this hypothesis.

The present work demonstrates the mixing of V/Si interface, induced by 120 MeV Au ions at fluences of $\sim 10^{13}$ - 10^{14} ions/cm² using two complimentary techniques like SIMS

and RBS. It is observed that the mixing is linearly dependent on the ion fluence. It is inferred that the cause of mixing is due to inter-diffusion across the interface during a transient melt phase according to the thermal spike model.

Depth profiling of the pristine (Fig. 1) and irradiated samples (Fig. 2) was performed by secondary ion mass spectroscopy (SIMS). The recorded SIMS profiles shown in the Figures clearly indicates mixing at the interface.

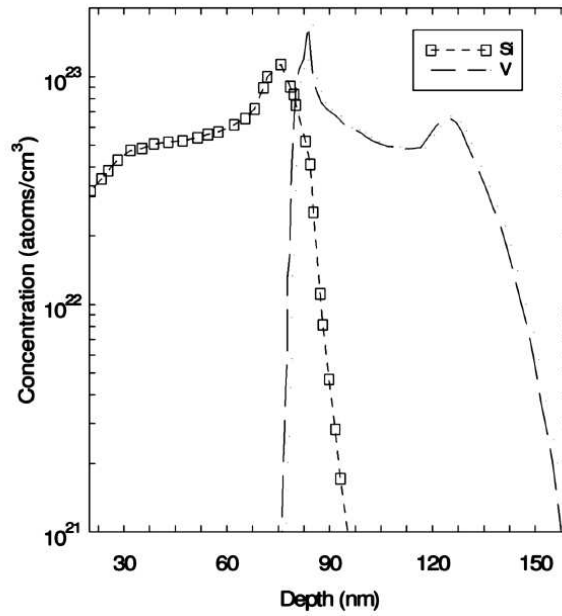


Fig. 1: SIMS depth profile of the pristine sample

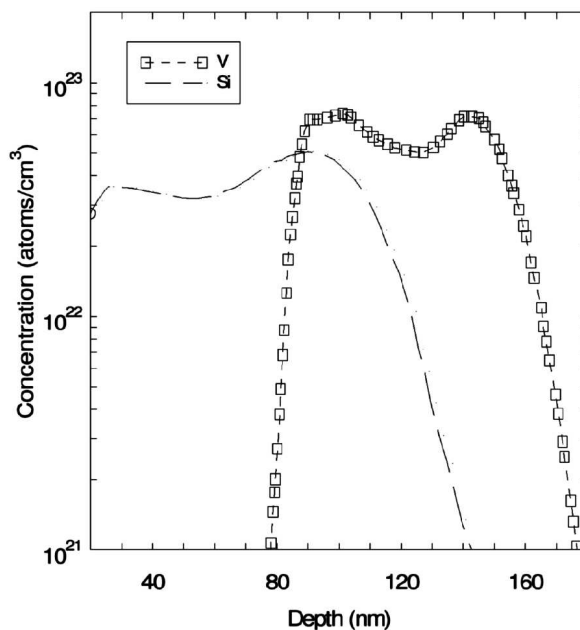


Fig. 2: SIMS depth profile of the irradiated sample (fluence 1×10^{14} ions/cm²)

REFERENCES

- [1] Y.T. Chang, Mat. Sci. Rep. 5 (1990)1.
- [2] C. Dufour, P. Bauer, G. Marchal, J. Grilhe, C. Jaouen, J. Pacaud and J.C. Jousset, Europhys. Lett. 21 (1993) 671.
- [3] W. Assmann, D.K. Avasthi, M. Doblere, S. Kruijjer, H.D. Mieskes and H. Nolte, Nucl. Instr. Methods B, (1998),146.
- [4] Z.G. Wang, C. Dufour, E. Paumier and M. Toulemonde, J. Phys. :Condensed Matter 6(1994) 6733.
- [5] D.K. Avasthi, W. Assmann, H. Nolte, H.D Mieskes, H. Huber, E.T. Subramaniam, A. Tripathi and S. Ghosh, Nucl. Instru. Meth. Phys. Res. B 166/167 (2000) 345.

5.2.3 Swift heavy ion induced formation of preferentially oriented Au_{0.6}Ge_{0.4} alloy

T. Som¹, B. Satpati¹, P.V. Satyam¹, P. Ayyub² and D. Kabiraj³

¹Institute of Physics, Sachivalaya Marg, Bhubaneswar - 751 005

²DCMP&MS, Tata Institute of Fundamental Research, Mumbai - 400005

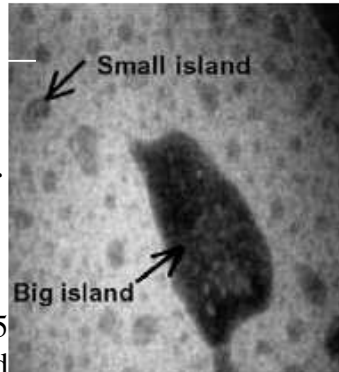
³Nuclear Science Centre, New Delhi - 110 067

Ion beam mixing using swift heavy ion (SHI) irradiation is a field of recent interest due to its fundamental importance. A very few works have been reported in this direction. In this work, we have studied the formation of nanometer dimensional seeds of Au_{0.6}Ge_{0.4} alloy following 120 MeV Au⁷⁺ irradiation at RT. We have also studied the formation of preferentially oriented Au_{0.6}Ge_{0.4} alloy by subsequent vacuum annealing.

Thin films of Au (42.5 nm) and Ge (38 nm) were deposited on Si (100) substrates by electron-beam evaporation technique. The films were irradiated at Nuclear Science Centre using 120 MeV Au⁹⁺ ions at room temperature at different fluences in the range of 1×10¹² to 1×10¹³ ions/cm². The beam was scanned over the entire surface area to get a uniform irradiation. The pristine as well as the irradiated samples were later vacuum annealed at 360°C for different time durations. We have characterized the samples by transmission electron microscopy (TEM). The results, however, were corroborated by XRD.

Although low magnification TEM image as well as the corresponding selected area diffraction (SAD) pattern indicated that the top Au layer remains polycrystalline, highly magnified TEM images showed the presence of small islands having average dimensions of 5-25 nm. High-resolution lattice imaging of many smaller and bigger islands confirmed

Fig. 1. Magnified TEM images and Au_{0.6}Ge_{0.4} nanoislands after 120 MeV Au⁷⁺ irradiation at 1×10¹³ ions/cm²



showing the presence of Au irradiation of Au/Ge bilayer with RT with a fluence of 1×10¹³

that the bigger ones (~20-25 nm) were Au, while the smaller islands belong to the mixed phase of Au_{0.6}Ge_{0.4}. No lattice imaging was obtained from the surrounding medium of the nanoislands since the image appeared to form an amorphous structure.

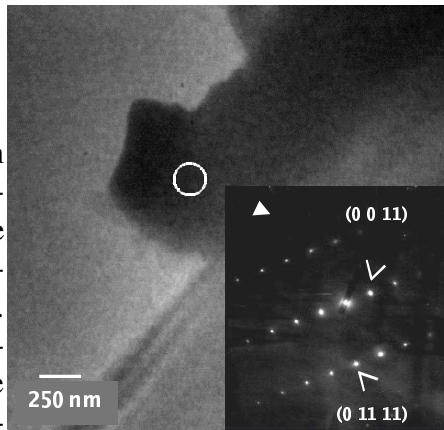
Since XRD studies did not show any Ge peak, it would be expected to be amorphous. Alternatively, the presence of an oxide layer between Au and Ge could not be ruled out either due to the operating vacuum under which Ge was deposited. Thus, one can infer that SHI irradiation of Au/Ge bilayer system leads to the formation of nano-dimensional seeds of Au_{0.6}Ge_{0.4} alloy although the other characterization techniques did not show any mixing.

As a next step, the irradiated samples were vacuum annealed at 360°C for different durations. As a result of annealing, new features came up in the sample microstructures as seen from TEM studies. Very clear μm-sized islands got created at the surface of the sample. XRD studies showed the formation of Au_{0.6}Ge_{0.4} phase with the presence of

only (800) reflection. This could be a possible indication for the formation of preferentially oriented big islands of $\text{Au}_{0.6}\text{Ge}_{0.4}$. To confirm the oriented nature of the Au-Ge alloy, we performed TEM studies and collected SAD patterns from one of the big isolated islands. The SAD pattern indeed shows the single crystalline nature as is clear from Fig. 2.

Fig.2. TEM planar micrograph taken from the μm -sized Au-Ge island structure. The inset shows the SAD pattern, which is indicative of oriented nature of the island.

The interdiffusion interface in a thermal environment is enhanced in similar conditions and at a temperature that melts at 360°C . over large areas of the specimen. In order to achieve energy, Au-Ge island formation is observed by TEM.



of Au and Ge across the environment is enhanced in sample annealed under conditions that maintains the eutectic composition. This leads to the dewetting phenomenon due to surface tension. The minimum surface energy condition takes place as observed by TEM.

Further, a natural cooling of the samples leads to the formation of Au-rich metastable Au-Ge alloy from a molten state as observed by XRD measurements.

5.2.4 Swift heavy ion induced interface modification in Co/Ge

T. Som¹, B. Satpati¹, P.V. Satyam¹, D. Kabiraj⁴, Ajay Gupta² and N.C. Mishra³

¹Institute of Physics, Sachivalaya Marg, Bhubaneswar - 751 005

²Inter-University Consortium for DAE Facilities, Khandwa Road, Indore 452 017

³Department of Physics, Utkal University, Sachivalaya Marg, Bhubaneswar - 751 004

⁴Nuclear Science Centre, New Delhi – 110 067

Metal/semiconductor based systems are good candidates for case study for ion beam mixing using swift heavy ion (SHI) irradiation due to the fundamental importance as well as wide applications. Recently, we have reported SHI induced Ni-Ge alloy formation. In this direction, we have taken up the SHI induced mixing study in Co/Ge system. In this work, we have studied the formation of a thin Co-Ge alloy phase by room temperature irradiation of Co/Ge bilayer films with 100 MeV Au ions up to a fluence of 1×10^{14} ions/cm².

Thin films of Au (42.5 nm) and Ge (34 nm) were deposited on Si (111) substrates using UHV electron-beam evaporation set-up. The films were irradiated at Nuclear Science Centre using 100 MeV Au⁷⁺ ions at room temperature (RT) and liquid nitrogen temperature (LT) with different fluences in the range of 1×10^{12} to 1×10^{14} ions/cm². The beam was scanned over the entire surface area to get a uniform irradiation. We have characterized the samples by Rutherford backscattering spectrometry (RBS) and cross-sectional transmission electron microscopy (XTEM).

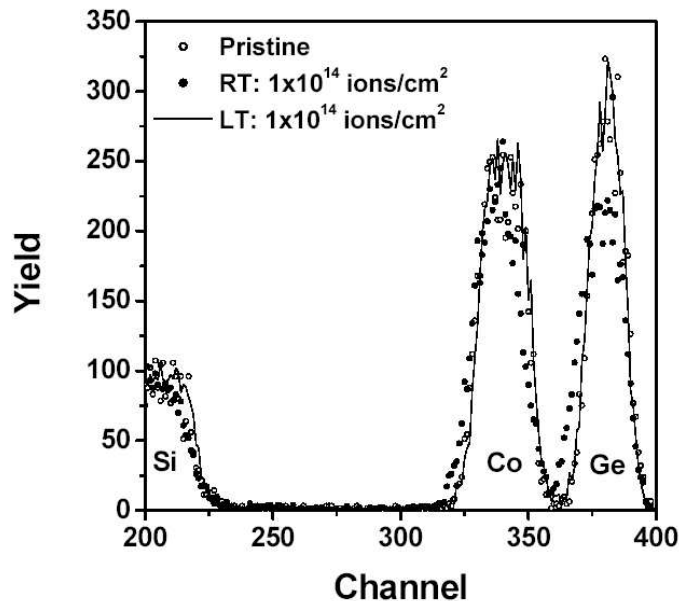


Fig. 1: RBS spectra of Ni/Ge bilayer structures: Pristine, 100 MeV Au irradiated at RT and LT

RBS analyses before and after RT irradiation of the Co/Ge bilayer structure showed mixing to take place (corresponding to the highest fluence), which is evident through the shift in the RBS peaks from the base line and a little shift (~10-12 keV) in the Co peak towards its surface position. This is accompanied by the broadening in the Ge signal, which could arise due to inhomogeneity in the Ge layer and/or incorporation of some impurity in the same. The results have been shown in Fig.1. On the other hand, almost no mixing is observed in case of LT irradiated sample.

XTEM measurements show the top layer of Ge to be amorphous, while the underneath Co layer is a polycrystalline one (Fig.2). XTEM micrograph collected from the RT irradiated sample shows a lot of non-uniformity in the top Ge layer (Fig.3(a)) with the formation of ~40-45 nm long void like structures with average width of ~10-12 nm. A small layer (~3-4 nm) forms between the polycrystalline Co and the Ge layer. High-resolution lattice image shows (Fig. 3(b)) that this layer is having a different orientation and grain size as compared to the Co layer. Calculations yield two different d-spacings of 0.270 nm and 0.215 nm, which closely match with the (310) and (311) planes of CoGe phase as well as (111) and (310) planes of Co₂Ge phase. Thus, it is difficult to unambiguously predict the Co-Ge alloy phase that is getting formed. However, invoking the concept of effective heat of formation rule, Co₂Ge is the most likely phase to form first.

Fig.2. XTEM micrographs of pristine Co/Ge bilayer: (a) low-magnification bright field image showing all the layers (with Ge as top layer) and (b) high resolution lattice image from the Co layer.

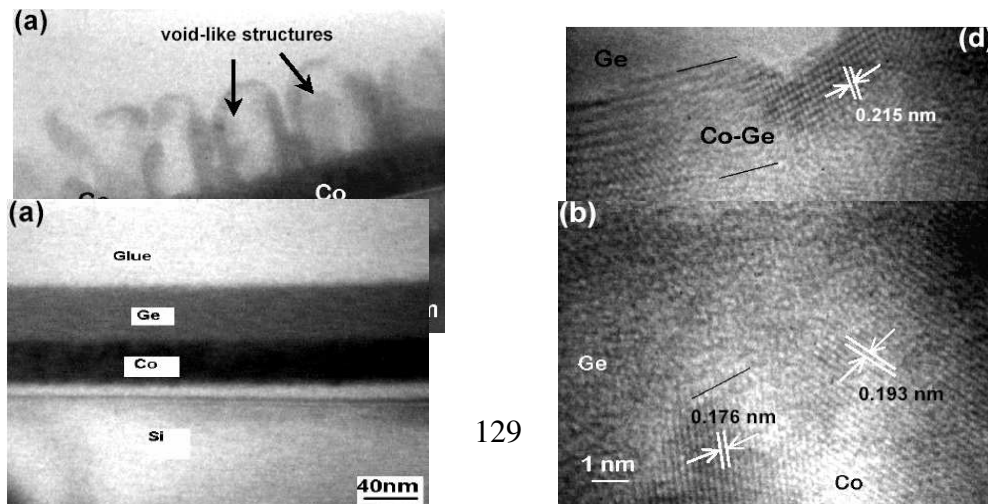


Fig. 3: XTEM micrographs of Co/Ge bilayer irradiated with 100 MeV Au (1×10^{14} ions/cm² at RT): (a) low-magnification bright field image showing all the layers and (b) high resolution lattice image from the mixed Co-Ge layer.

We attribute the feature observed in the Ge layer to the swift heavy ion (SHI) irradiation induced variation in local density. At the same time, it would be expected to see a large scale change in the Co layer since the threshold value of electronic energy loss (S_e) for defect creation in bulk Co is quite close to the present S_e value. However, Co layer retained its crystallinity after RT irradiation.

So far the mixing is concerned, it should be mentioned here that the irradiation fluence is quite high compared to the defect overlap regime (typically 5×10^{12} ions/cm²) and so it is unlikely that S_e alone is contributing to the mixing process. As a matter of fact, nuclear energy loss (S_n) being close to the value corresponding to low energy Ar ion induced mixing in Co/Ge system, where Co-Ge alloy phase formation was reported earlier (at a fluence of 1×10^{16} ions/cm²), it is expected that S_n may also contribute to the observed mixing here. However, in the present case, fluence being less by two orders of magnitude, displacement per atom (dpa) will be very less in both the layers and hence it will not be sufficient to move the required amount of material to lead to atomic mixing. Therefore, it seems that both S_e and S_n are operating in a synergetic manner to create the mixing. It can be explained in the following way. It is quite obvious that a large number of point defects will be created near the Co interface and since S_n induced effects are cumulative in nature, this will lead to significant atomic movement during the formation of the S_e mediated thermal spike. This synergy will observe atomic movements across the *highly* reactive Co-Ge interface to cause mixing. For LT irradiation, less atomic mobility leads to lesser amount of mixing.

5.2.5 Atomic Transport in Cu/Ge System at Interface by Swift Heavy Ions

Sarvesh Kumar¹, R.S. Chauhan¹ and D.K. Avasthi²

¹Department of Physics, R. B. S. College, Agra-282 002

²Nuclear Science Centre, New Delhi-110 067

High-energy heavy ions with velocities comparable to or higher than the orbital electron velocity are referred to as swift heavy ions (SHI). At such energies (\geq a few tens of keV/nucleon) SHI lose their energy in the target mainly via inelastic collision leading to the excitation of the target electrons. Avasthi et al. [1] irradiated CuO thin film on float glass with 210 MeV I ions and suggested that the diffusion of oxygen across the interface takes place during the transient melt phase. Srivastava et al. [2] concluded that mixing

takes place at the interface by observing the decrease in the resistivity of the Fe/Ni multilayer after irradiation with 120 MeV Au ions, a result of homogenization of the disordered multilayer structure. Kumar et al. [3] investigated the ion beam mixing in Cu/Ge bilayer system using 120 and 140 MeV Au ions and found that mixing increases with the fluence and with the electronic energy loss. Ion beam mixing by SHI is investigated in a very limited number of cases and therefore only little is known about atomic transport processes within the highly excited nuclear tracks of high-energy ions. In the present work, we report the in-situ resistivity measurement for Cu/Ge multilayer system using 120 MeV Au ions at room temperature (RT) and correlate it with atomic transport at interface.

The multilayer, [Ge(129Å)/Cu(203Å)]x5, is deposited onto Si (100) substrate by sequential evaporation of Ge by electron gun and Cu by resistive heating, at room temperature in the ultra high vacuum deposition system without breaking the vacuum after deposition of each layer. The pressure during deposition was $\sim 2 \times 10^{-7}$ Torr. The substrates were cleaned and etched by usual procedure before deposition. The in-situ resistivity is measured by using van der Pauw four-point probe method. Irradiation by 120 MeV Au ions was carried out using 15 UD Pelletron accelerator at Nuclear Science Centre, New Delhi.

In-situ measurement resistivity versus fluence is shown in Fig. 1. The resistivity increases from the pristine value ($\sim 47.55 \mu\Omega\text{-cm}$) to ($\sim 54.00 \mu\Omega\text{-cm}$) up to the fluence of 2.8×10^{13} ions/cm². From Cu-Ge phase diagram [4] we know that as the percentage of Ge in Cu-Ge system increases, the resistivity also increases. Thus the increase in resistivity with the increasing fluence indicates that the atomic transfer takes place at the interface suggesting a mixing of Cu and Ge atoms at interface.

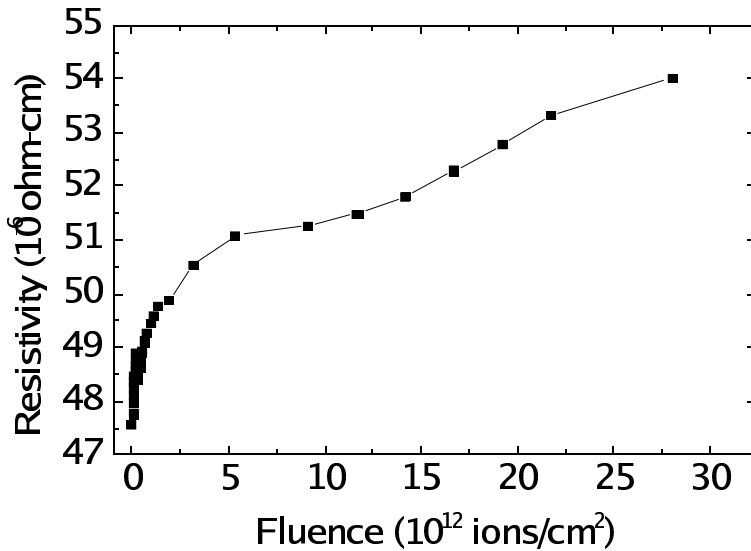


Fig. 1: In-situ resistivity of Cu/Ge multilayer with fluence using 120 MeV Au ions at RT

REFERENCES

- [1] D.K. Avasthi, W. Assmann, H. Nolte, H.D. Mieskes, S. Ghosh and N.C. Mishra, Nucl. Instr. and Meth. Phys. Res. **B 166-167** (2000) 345.
- [2] S.K. Srivastava, Ravi Kumar, S.K. Arora, D. Kabiraj, D. Bhattacharya, R.S. Patel, A.K. Majumdar, A. Gupta and D.K. Avasthi, DAE-SSPS **43** (2000) 360.
- [3] Sarvesh Kumar, R.S. Chauhan, R.P. Singh, D. Kabiraj, P.K. Sahoo, C. Rumbolz, S.K. Srivastava, W. Bole and D.K. Avasthi, Nucl. Instr. and Meth. Phys. Res. B **212** (2003) 242.
- [4] Klaus Schroder, CRC Handbook of Electrical Resistivities of Binary Metallic Alloys (1983).

5.2.6 Swift Heavy Ion Induced Modification of Si/C₆₀ Multilayers

S.K. Srivastava¹, D. Kabiraj³, B. Schattat², H.D. Carstanjen¹ and D.K. Avasthi³

¹Max-Planck-Institut für Metallforschung, Heisenbergstr. 3, Stuttgart, Germany

²Institut für Strahlenphysik, Universität Stuttgart, Germany

³Nuclear Science Centre, New Delhi-110067

Currently, there is an increasing drive in the scientific community to reduce the synthesis temperature of thin SiC films, which have alluring superior properties. Although mixing of Si and C has been reported by low energy ion beam mixing [1] at room temperature (RT), no phase formation has been demonstrated. The well known capability of SHI to produce high temperature (HT) conditions (latent tracks) in matter makes it more interesting to use SHI mixing of Si/C-allotrope multilayer for SiC synthesis which requires HT conditions. Based on the recent reports on SiC production by carbonization of C₆₀ on Si substrates at 800 to 1000 °C temperatures [2] and the capability of SHI to produce multi-fragmentation of C₆₀ [3] apart from the creation of HT conditions, we investigate in this report the synthesis of 4H-SiC by RT irradiation of Si/C₆₀ multilayers by 120 MeV and 350 MeV Au ions.

Sequentially electron beam evaporated thin [Si/C₆₀]_{x5} multilayers, deposited on a Si substrate kept at RT, were irradiated at RT by 120 MeV Au at NSC, New Delhi and by 350 MeV Au at HMI, Berlin at a fluence of 1×10^{14} ions/cm². The electronic (nuclear) energy losses are ~ 13.3 (~ 0.2) keV/nm and ~ 19.0 (~ 0.1) keV/nm for the two ions respectively. Characterizations were done by high resolution Rutherford backscattering (HRBS) spectrometry at MPI-MF, Stuttgart. Atomic force microscopy (AFM) and X-ray diffraction (XRD) were also performed at MPI-MF, Stuttgart to examine the irradiation induced surface roughness and phase formation, respectively. The HRBS spectra were fitted by SIMNRA code.

The HRBS spectra of the backscattered particles from Si for pristine and 120 MeV and 350 MeV Au irradiated samples are shown in Fig. 1. The corresponding SIMNRA fits are shown in Fig. 2.

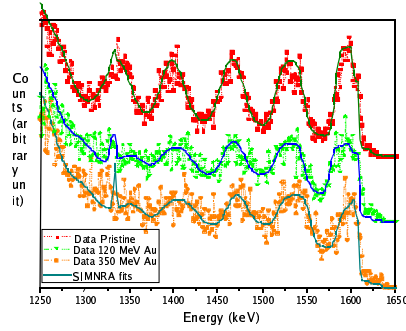


Fig.1. HRBS spectra of pristine and 1×10^{14} ions/cm² 120 MeV and 350 MeV Au irradiated samples. The experimental data are shown by symbols+broken lines. The continuous lines are the corresponding SIMNRA fits.

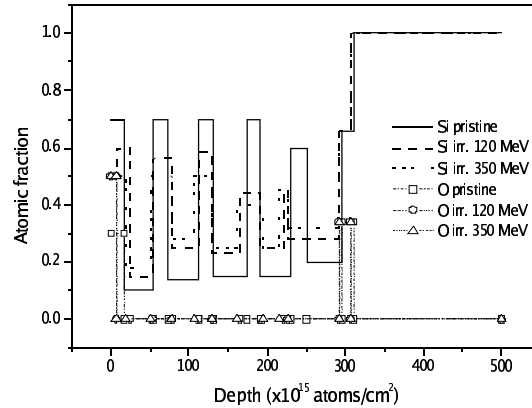


Fig.2. SIMNRA Depth profiles of Si concentration (lines) for pristine and 1×10^{14} ions/cm² 120 MeV and 350 MeV Au irradiated samples. It is evident that oxygen (line+symbol) stays at the sample surface and sample/substrate interface.

There are four main observations:

- 3 Significant amount of interdiffusion across Si/C₆₀ interface shown by HRBS and formation of 4H-SiC phase as identified by XRD. The observation has been explained on the basis of thermal spike model (TSM). The formation of latent (molten) tracks in C₆₀, composed of its fragments, as predicted by the model has been shown previously [3]. The radii and duration of melt phase are 6 nm and 10-100 ps, respectively. Similar transient HT conditions exist also in the Si layers. Thus, C₆₀ fragmentation and HT conditions are simultaneously achieved to synthesize SiC.
- 4 The amount of intermixing and the fraction of SiC phase are more in the case of 350 MeV irradiation than those in the case of 120 MeV irradiation. This is

in conformation with the TSM, according to which, higher electronic energy loss of 350 MeV Au ions leads to higher latent track radius and longer melt duration, leading to higher amount of intermixing.

- 5 The interdiffusion coefficient of Si in C, considering the mixing to take place in the transient molten state, comes out to be $\sim 10^{-8} - 10^{-9} \text{ m}^2/\text{s}$. This is of the order of liquid state diffusivities and the postulation of molten state diffusion is also verified.
- 6 The amount of intermixing for both the ions increases with the multilayer depth. This has been explained in the following way. In the first stage of the distribution of the SHI deposited energy in the electronic subsystem, about two-third is used up in the production of δ - and convoy electrons with average velocities equal to and twice that of the ion velocity, respectively. Deeper layers have additional contribution in heating (due to electron phonon coupling) from the electrons generated in the near surface layers.

In conclusion, it has been shown that RT 120 MeV and 350 MeV Au ion irradiation at $1 \times 10^{14} \text{ ions/cm}^2$ fluence induce considerable intermixing at Si/C₆₀ interface to form 4H-SiC phase. The amount of mixing increases with depth and electronic energy loss. The requirement of HT conditions for this to take place proves the applicability of the TSM as the responsible mechanism. The high diffusivity establishes that the mixing is due to an interdiffusion in transient melt phase.

REFERENCES

- [1] F. Harbsmeier, W. Bolse and A.-M. Flank, Nucl. Instr. Meth. Phys. Res. B **166-167** (2000) 385.
- [2] A.V. Hamza, M. Balooch and M. Moalem, Surface Science **317** (1994) L1129.
- [3] S. Lotha, A. Ingale, D.K. Avasthi, V.K. Mittal, S. Mishra, K.C. Rustagi, A. Gupta, V.N. Kulkarni and D.T. Khathing, Solid State Comm. **111** (1999) 55.

5.2.7 Phase Transformations in Thin Films of C₆₀ Irradiated with 100 MeV Au ions

Keya Dharamvir¹, Navdeep Bajwa¹, V.K.Jindal¹, D.K.Avasthi³, Ravi Kumar³, A.Tripathi³ and Alka Ingale²

¹Department of Physics, Panjab University, Chandigarh

²Center for Advanced Technology, Indore

³Nuclear Science Center, New Delhi-110067

Thin films of C₆₀ were irradiated with 100 MeV Au ions. Films of C₆₀ with a thickness of 230nm were deposited on Si and quartz substrates using resistive heating method in a high vacuum of 2×10^{-6} Torr with substrate temperature kept at room temperature. The thickness of the thin films was kept very small as compared to the range of the

ion used. The changes induced in the films were investigated using Raman spectroscopy, optical absorption spectroscopy and temperature dependent resistivity measurements.

Raman spectra of pristine and irradiated C₆₀ films were recorded using Raman spectrometer, LABRAM with 5145Å at Institut für Physikalische Chemie, Germany. Fig. 1 shows Raman spectra of pristine and some irradiated C₆₀ films. The Raman spectrum of pristine C₆₀ shows the characteristic modes [1] of C₆₀ molecule – at 1420 cm⁻¹ (H_g mode), 1465 cm⁻¹ (A_g) and 1570 cm⁻¹ (H_g). With increase in fluence, asymmetry is seen to develop around the prominent peak (1465cm⁻¹) which starts at the first fluence. This asymmetry-producing peak (1458 cm⁻¹) has been identified [2] as one due to the dimerized / polymerized C₆₀. Fig. 2 shows the trend of this peak as observed for Au irradiated C₆₀ thin films, with increase in fluence. It can be clearly seen that this peak first increases, optimizes at a fluence of 3x10¹¹ ions/cm², then declines and ultimately vanishes at high fluence [3]. This peak as well as those of C₆₀, vanish almost at the same fluence. High fluences lead to amorphous carbon formation. Emergence of three broad peaks is seen. One around 1380 cm⁻¹ (D peak), one around 1566 cm⁻¹ (G peak) [3,4] indicating formation of amorphous carbon and the third around 1445 cm⁻¹. In addition to these two more peaks are also observed, one around 1230cm⁻¹ and the other around 1090cm⁻¹. These features are being studied for proper identification.

Optical absorption measurements were performed on pristine and irradiated C₆₀ films, using U3300 Hitachi spectrophotometer at NSC. The optical data was used to determine the band gap. The high fluence irradiated C₆₀ samples have bandgaps which are too low to be obtained from the optical absorption spectroscopy. Hence they were determined using temperature dependent resistivity measurements to obtain a semiconducting gap using the hopping conduction model.

$$R = R_0 \exp(-E_g / 2k_B T)$$

here R is the resistance of a semiconducting sample and E_g is the band-gap. A plot of $\ln(R/R_0)$ vs. $1/T$ (called Arrhenius plot), determines the bandgap. Fig. 3 shows a plot of bandgap variation with increase in fluence for Au irradiated C₆₀. The data includes bandgap values obtained from both optical absorption spectroscopy as well as temperature dependent resistivity measurements.

The results of Raman spectroscopy, optical absorption spectroscopy and temperature dependent resistivity measurements are consistent. Earlier we have worked with Ni and O ions and the results obtained using the above measurement techniques show similar trends and features. Thus we conclude that the phase transformations taking place in C₆₀ thin films due to the different ions, have a strong correlation with the S_e value and fluence. This correlation determines when the various phases come into existence or optimize. Lower the S_e, higher is the fluence required for onset of conductivity. Similarly, for closing of band gap and optimum dimer formation, higher fluence is required for ions with lower S_e.

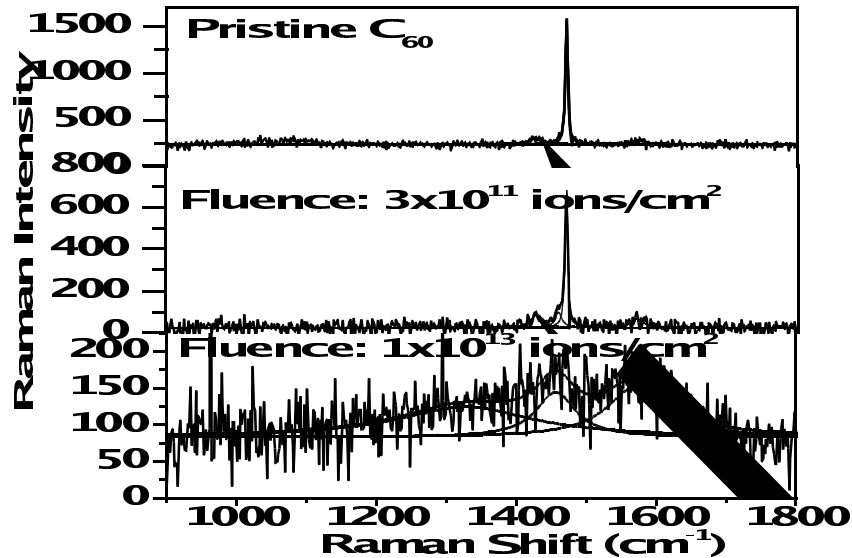


Fig.1: Raman spectra of pristine and some Au irradiated C_{60} thin films.

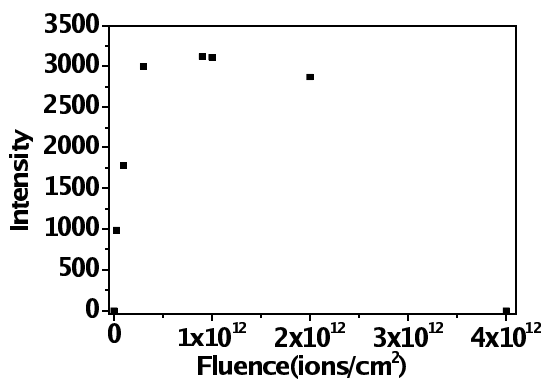


Fig. 2: Plot showing trend of polymer peak with increase in fluence for Au irradiated C_{60} thin films.

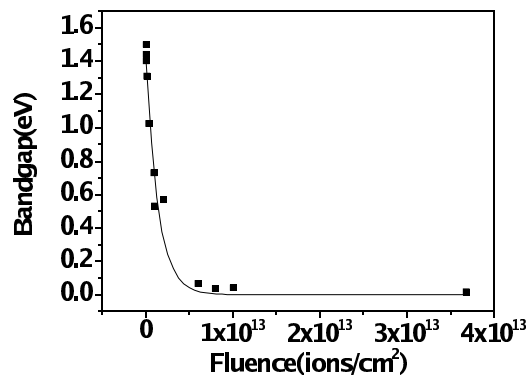


Fig. 3: Plot showing variation of bandgap with fluence for Au irradiated C_{60} thin films. The solid line shows exponential fitting.

REFERENCES

- 7 Z.H.Dong, P.Zhou, J.M.Holden, P.C.Eklund, M.S.Dresselhaus and G.Dresselhaus, Phys. Rev.B, **48**, 2862 (1993).
- 8 S.Lotha, A.Ingale, D.K.Avasthi, V.K.Mittal, S.Mishra, K.C.Rustagi, A.Gupta, V.N.Kulkarni and D.T.Khathing, Solid State Communications **111**, 55 (1999).
- 9 N. Bajwa, A. Ingale, D.K.Avasthi, Ravi Kumar, K.Dharamvir and V.K.Jindal, communicated to J. App. Phys. 2003.
- 10 A.C.Ferrari and J.Robertson, Phys. Rev. B **64** 075414 (2001) and references therein.

5.2.8 Luminescence from Silicon Nanophases Grown in Fused Silica using keV and MeV Ion Beam

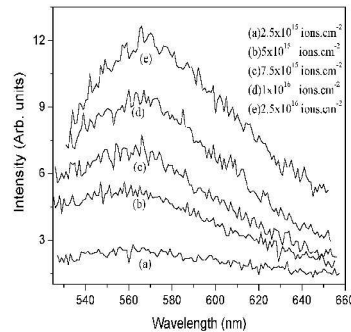
T. Mohanty³, Asima Pradhan¹, N.C. Mishra² and D. Kanjilal³

¹Physics Department, I.I.T. Kanpur-208 016

²Physics Department, Utkal University, Bhubaneswar-751 004

³Nuclear Science Centre, New Delhi-110 067

Formation of Si-nanoclusters has opened a new era in optoelectronic industry. Silicon nanocrystals can emit red, green and even weak blue light of shorter wavelength. The key issue in the growth process is to synthesize Si-nanocrystals in an insulating matrix, preferably SiO₂ films with a narrow size distribution. This would enable one to increase the band gap of Si from 1.1 to 4 keV in small increment energies by decreasing the particle size in small steps allowing wide range applications of Si as detectors, light emit-



ting devices from infrared to visible UV radiation. In this work, detail studies on precipitation of Si-nanoclusters in SiO₂ using SHI irradiation in MeV energy range are reported. Nanoprecipitation is expected to occur along the SHI induced track as well as in tubular area surrounding the track. Silicon nanocrystals are grown on fused silica using both keV and MeV ion beam followed by annealing. Initially 200 keV Si⁺ ions from ECR ion source were implanted in optical grade fused silica at various fluences upto 2.5×10^{16} ions/cm².

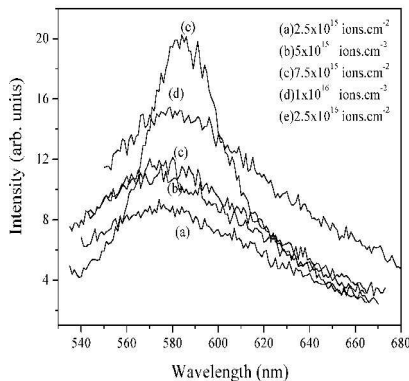


Fig. 1: PL spectra of implanted annealed samples

Fig. 2: PL spectra of implanted, SHI irradiated and annealed samples

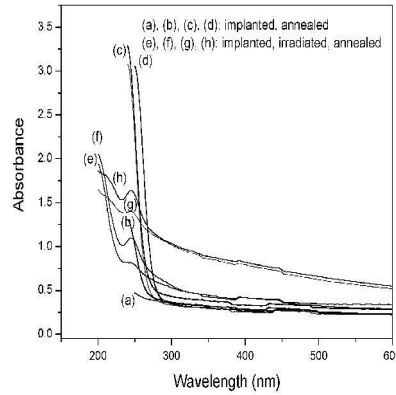


Fig. 3: Absorption spectra of Si nanoparticles grown by thermal and athermal Annealing

- (a), (e) : 5×10^{15} ions.cm⁻²,
(c), (g) : 1×10^{16} ions.cm⁻²
(b), (f) : 7.5×10^{15} ions.cm⁻²
(d), (h) : 2.5×10^{16} ions.cm⁻²

The projected range of the ion implantation ~ 300 nm calculated by using the TRIM 98 code. Both annealing at high temperature and athermal annealing using swift heavy ion beam were carried out for nanoprecipitation to occur. One set of implanted samples were annealed at 1050 C in N₂ atmosphere for 3 hours. Other set of the implanted samples were irradiated using 70 MeV Si beam from 16 MV Pelletron Tandem accelerator. The irradiated samples were annealed at 900C for 3h in nitrogen atmosphere. The annealed samples along with pristine sample were characterized by UV/VIS optical absorption spectroscopy, PL measurement. PL spectra were taken using 514 nm line of Argon ion laser.

Photoluminescence (PL) spectra were taken (Figures 1 and 2) for both sets of samples. Implanted and annealed samples had PL peak at 580 nm whereas implanted, irradiated and annealed samples showed PL peak at 568 nm [1]. The PL peak corresponding to these wavelengths does not come from defects [2]. The blue shift observed in PL is attributed to quantum size effect in which reduction of the average nanocrystal size leads to emission at a shorter wavelength.

The formation of Si nanocrystals has also been confirmed by complementary studies of UV-visible absorption spectra (Figure 3). Blue shift of absorption edges is observed for samples irradiated with 70 MeV Si beam.

It is expected that nanoclusters are grown inside the tracks of ~ 1 nm radius [4] when swift heavy ion irradiation induced annealing is done. Tracks act as capping agent for the growth of nanoclusters thus restricting their size to diameter of the track.

REFERENCES

- [1] T. Mohanty, N.C. Mishra, Asima Pradhan, D. Kanjilal, presented at 13th International Conference on surface modification of materials by Ion beam SMMIB 2003 held at San Antonio, Texas, USA.
- [2] T. Mohanty, N.C. Mishra, P.K. Basu, S.V. Bhat and D. Kanjilal, J.Phys.D, Appl. Phys. 36 (2003) 3151
- [3] E. Valentin, H. Bernas, C. Ricolleau and F. Creuzet, Phys. Rev. Lett. 86 (2001) 99.
- [4] T. Mohanty, P.V. Satyam, N.C. Mishra and D. Kanjilal, Rad. Meas. 36 (2003) 137

5.2.9 Swift Heavy Ions induced Modifications IN ZnO thin films

P. M. Ratheesh Kumar¹, C. Sudha Kartha¹, K. P. Vijayakumar¹, F. Singh³, D. K. Avasthi³ and G. S. Okram².

¹Department of Physics, Cochin University of Science and Technology, Kochi-682 022

²Inter-University Consortium for DAE facilities, University Campus, Khandwa Road, Indore-452 001

³Nuclear Science Centre, New Delhi-110 067

Highly transparent ZnO thin films were prepared using Chemical Spray Pyrolysis (CSP) technique. Thickness of the samples was measured using Stylus method and was found to be 0.54 μm . Films of about 1 cm^2 area were irradiated using 120 MeV Au ion with fluences 1×10^{12} , 3×10^{12} , 1×10^{13} and 3×10^{13} ions/ cm^2 where modifications are expected mainly due to electronic excitation. Irradiation was done using 15UD Pelletron tandem accelerator at Nuclear Science Centre, New Delhi. Irradiated films were characterized using different techniques.

Intensity of the peak corresponding to the plane (002) decreases with ion fluence. Height of small peaks corresponding to the planes (101) and (103) were also found to decrease with ion fluence and vanishing completely at the ion fluence of 1×10^{13} ions/ cm^2 . Grain size of the films was found to be decreasing with the ion fluence. It is found that due to irradiation, only grain size is affected. From these observations, it may be concluded that the grain size of ZnO film is getting smaller and is slowly amorphized due to heavy ion irradiation.

Optical absorption of the samples, in the wavelength range 350 to 900 nm, was studied. It is to be specifically noted that there is no observable change in the values of band gap due to irradiation, implying that the basic crystal lattice of ZnO is not modified. This is in agreement with the structural results. Optical transmission spectra of the samples were recorded in the wavelength range 350-900 nm. Pristine sample shows 80-90 % transmit-

tance in the visible region and above 90 % in near IR region. Reduction in optical transmittance due to irradiation may be resulting from the formation of metal rich regions in the film.

Electrical resistivity of all samples were measured using four-probe method and interestingly, it was found to be decreasing with increase in the ion fluence. ZnO is an n-type semiconductor in which donor levels are due to oxygen vacancies (V_o) and interstitial zinc (Zn_i) atoms. So one can assume that the reason for decrease in resistivity may be due to the creation of oxygen vacancies (V_o) and zinc interstitial (Zn_i) during the irradiation with swift heavy ions.

Generally it is expected that the resistivity may increase due to decrease in the grain size and also due to increase in the grain boundary scattering. But the evolution of metallicity is also observed here that competes with earlier described phenomena. Hence we can say that the evolution of metallicity is dominating the grain boundary scattering effects and this enhances the conductivity. Carrier concentration was found to be increasing with the ion fluence. This gives additional support to the formation of metal rich oxide films due to irradiation.

PL measurements were done at room temperature. All samples showed characteristic peak at 517 nm, which corresponds to the blue green emission. These emissions were found to be extremely broad and this broadening may be due to phonon-assisted transition. Intensity of PL spectra was found to decrease with ion fluence. Center responsible for blue green emission in ZnO has not been completely understood. It has been suggested that this peak is associated with copper impurities at a substitutional positions, oxygen vacancies, and porosity of the films. However more recently it has been proposed that blue green emission in this material might be related to a transition within a self-activated centre formed by doubly ionized zinc vacancy (V_{Zn}^{-2}) and the ionized interstitial Zn_i or two nearest interstitials [1]. It has also been reported that the origin of green emission was due to the electronic transition from the bottom of the conduction band to the antisite defect O_{Zn} level [2]. In the case of our undoped ZnO samples, no intentional copper doping was made.

Using full-potential linear muffin –tin orbital method, the energy levels of intrinsic defects were calculated. It is found that energy interval from bottom of the conduction band to O_{Zn} level is 2.36 eV, which was in good agreement with the energy of green emission of PL observed in our experiment. As the ion fluence increases we observed a decrease in the integral intensity of the PL spectra. It might be due to the fact that as the ion fluence increases, this level due to the antisite oxygen is getting depleted from the sample.

REFERENCES

- [1] P. S. Xu, Y. M. Sun, C. S. Shi, F. Q. Xu and H. B. Pan, Nucl. Instrum. Methods. Phys. Res. B, **199**, 286 (2003)
- [2] Bixia Lin, Zhuxi Fu and Yunbo Jia, Appl. Phys. Lett. **79**, 943 (2001).

5.2.10 Electronic conduction in 40 MeV $^{28}\text{Si}^{5+}$ ion irradiated Se-Te-Pb thin films

Maninder Singh Kamboj¹ R. Thangaraj¹ and D.K. Avasthi²

¹Semiconductors Laboratory, Department of Applied Physics, Guru Nanak Dev University, Amritsar-143005

²Nuclear Science Center, New Delhi-110067

Chalcogenide glasses are interesting candidates for technological applications such as switching and memory devices, reversible phase change optical recordings, optical imaging and infrared optical fibres [1, 3]. These glasses also exhibit many properties like photodoping, photocrystallisation, photodarkening and photobleaching, [4]. They exhibit wide variety of changes in their structural properties, electronic transport properties and optical properties when they are exposed to light or heavy ion irradiation [5,6]. Their structure consists of a disordered network having some dangling bonds as defects [1]. High purity elements [99.999%] obtained from Sigma- Aldrich USA were used for the synthesis of bulk samples. The elements in appropriate amounts were sealed in a quartz ampoule in a vacuum of the order of 10^{-5} mbar. Then the ampoule was placed in a vertical furnace at 700°C and it was frequently inverted in order to ensure the homogeneous mixing of the constituents. After 48h it was quenched in an ice water bath. Using this as source material, thin films for all the compositions were prepared onto well-cleaned glass substrates at room temperature by thermal evaporation in a pressure less than 10^{-5} m-bar. Amorphous nature of the films was confirmed by the absence of any sharp peak in the X-ray diffraction (XRD) pattern. The composition analysis of the films was performed using Rutherford Back Scattering (RBS) technique. The films were irradiated at room temperature with 40 MeV $^{28}\text{Si}^{5+}$ ion beam for the RBS experiment. A silicon surface barrier detector (having a depletion depth of $60\ \mu\text{m}$) was used at back angle ($\sim 120^{\circ}$) to detect the Si ions back scattered from the sample. Since the masses of the constituents (Se, Te and Pb) are quite apart, the back-scattered Si ions appear in three groups well separated from each other, representing three different masses. The area of the peaks and Rutherford scattering cross section were used to determine relative concentration of Se, Te and Pb. The composition was verified at different parts of the films and was found to be uniform.

Thin films of about $1.0\ \text{cm}^2$ area were exposed to 40 MeV $^{28}\text{Si}^{5+}$ ion beam using 15UD NSC Pelletron New Delhi at fluences (10^{12} , 3×10^{12} , 10^{13} and 5×10^{13} ions/ cm^2). The DC electrical conductivity of the films was determined in the temperature range 220-313 K. Electrical contacts (with electrode gap $\sim 10^{-3}$ m) in a coplanar geometry were made using silver paint. The straight line passing through the origin of the voltage-current plot verified the Ohmic nature of the contacts. The DC current was noted by using a digital picoammeter (DPM-111 Scientific Equipments, Roorkee). It was noted that the DC electrical conductivity increases with the increase in temperature as well as with increase in irradiation fluence from 10^{12} to 5×10^{13} ion/ cm^2 . The DC conductivity is found to be activated over the entire range of temperature.

REFERENCES

- [1] Morigaki K, Physics of Amorphous Semiconductor, (Imperial College Press, London, 1999).
- [2] Tanaka Ke, Rev. Solid State Sci 1990; 4: 641.
- [3] Kamboj MS, Thangaraj R, Avasthi DK, Kabiraj D, Nucl Inst Meth Phys Res B 2003;211: 369.
- [4] Owen AE, Firth AP, Ewen PJS, Philos Mag B 1985;52:347.
- [5] Kamboj MS, Kaur G, Thangaraj R, Avasthi DK, J Phys D: Appl Phys 2002; 35: 477.
- [6] Bhatia KL, Singh P, Kishore N, Malik SK, Philos Mag B 1995;729: 413.

5.2.11 Studies on 150 MeV Ni¹¹⁺ Ions Irradiated Nanocrystalline Li Ferrite Thin Films

Sanjukta Ghosh¹, S. A. Khan⁴, S. Kundu², V. R. Reddy³ and A. Gupta³

¹Department of Physics, University of Calcutta, 92 A.P.C. Road, Kolkata-700009

²Saha Institute of Nuclear Physics, 1/AF Bidhannagar, Kolkata-700 064

³Inter University Consortium, Khandwa Road, Indore-452 017

⁴Nuclear Science Centre, New Delhi-110 067

To probe the swift heavy ions (SHI) induced modifications in Li_{0.5}Mn_{0.1}Fe_{2.4}O₄ ferrite thin films around the threshold value of the electronic energy loss (S_e), we have irradiated the films with 150 MeV Ni¹¹⁺ ions. The S_e value has been calculated from the TRIM program. The preparations of the films have been carried out using R. F. magnetron sputtering system. It is worth mentioning that the applications of ferrite thin films in our modern technology are increasing also due to their SHI induced interesting aspects. Presently we emphasize on the same electrical and magnetic properties. In-situ measurement on resistivity has not shown any drastic changes and this picture is also nearly same for magnetic properties. It can be clearly stated that the meager changes shown in Figure 1 arises due to point defects or extended defects. We are carrying on further analysis.

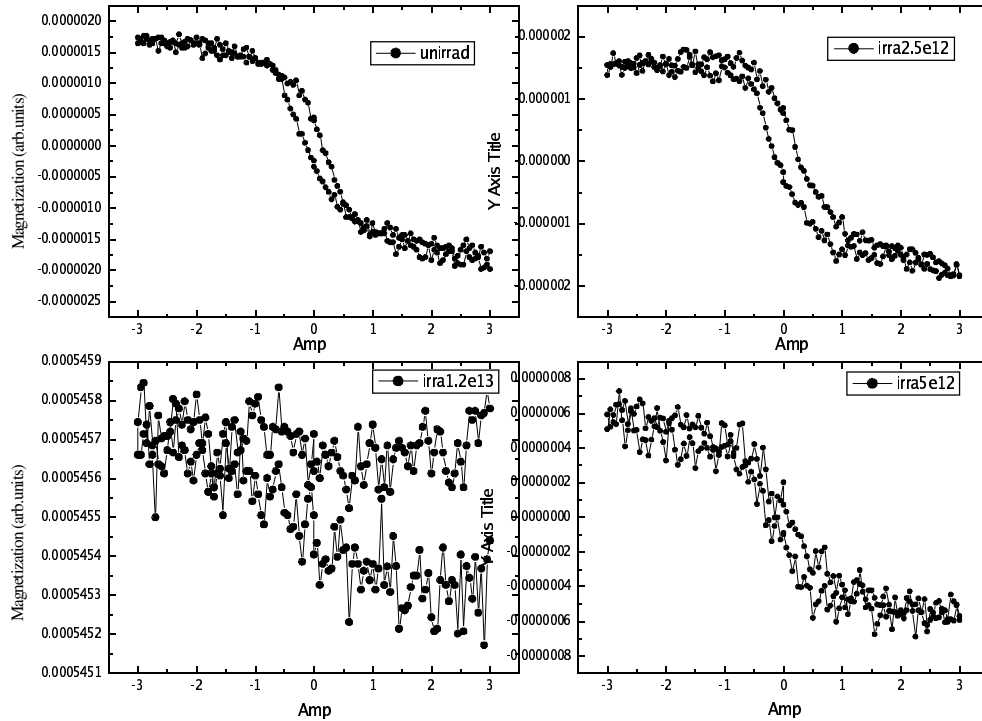


Fig. 1: Magnetization (a. u) versus fluence when irradiated with 150 MeV Ni¹¹⁺ ions

5.2.12 80 MeV Silicon Ion Irradiation Effects in GaN & II-VI Compound Semiconductors

S. Soundeswaran¹, E. Varadarajan¹, O. Senthil Kumar¹, D. Kabiraj², D.K. Avasthi², and R. Dhanasekaran¹

¹Crystal Growth Centre, Anna University, Chennai – 600 025

²Nuclear Science Center, New Delhi - 110067

II-VI and III-V compound semiconductors are important for the fabrication of many optoelectronic devices. Compounds like CdS and GaN are having wide bandgap in the visible region. CdS thin films were prepared using chemical bath deposition and photochemical deposition methods, ZnSe by electrocrystallisation technique and GaN by Vapour Phase Epitaxial method. Irradiation of these materials by high-energy ions may create some complex defects and in some cases result in forming the luminescent centers. Si ion irradiation of CdS and GaN has been carried out. Si ion irradiation was performed with energy of 80 MeV at a current density of 3 pA/cm² of fluences 1 x10¹¹, 1 x10¹², 2 x10¹³, 2 x10¹⁴, and 1 x10¹⁴ using Tandem Pelletron Accelerator.

Unintentionally doped n-type wurtzite GaN epitaxial layers of 4 μm thick, epitaxially grown on sapphire (0001) substrate by VPE technique were taken for the experiment. n-type CdS thin films of 3 μm thick, grown on galss substrate by Photo-Chemical Depos-

ition technique and Chemical Bath Deposition technique and ZnSe thin films and CdS thin films prepared by electrochemical deposition technique were taken for the experiment. The samples were cut into several numbers of small pieces of dimensions about 5 mm x 5 mm to be used for irradiation.

Ex-situ optical measurements have been carried out for various doses of ion irradiation. Raman analysis has been performed on the as-grown and irradiated GaN samples (Figure 1). Due to compressive and dilative strain there was a change in the Raman modes. New peaks are also observed due to high energy irradiation at high dose. Optical absorption spectra was recorded (Figure 2) and the bandgap value of the GaN samples decreases from 3.4 eV to 2.99 eV. Thus, the high energy Si ion radiation can be considered as an effective process for optical isolation of GaN epitaxial layers [1,2].

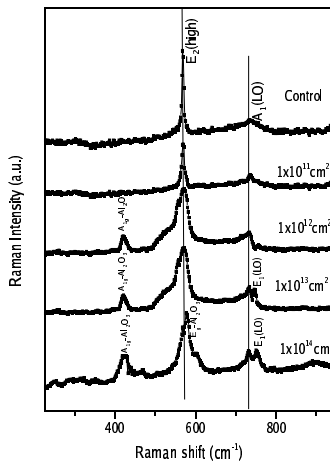


Fig. 1 The room temperature Raman spectra of as-grown and Si ion irradiated GaN epilayers

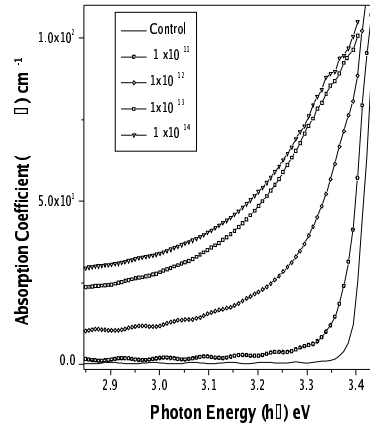


Fig. 2 Absorption coefficient versus energy plot of as-grown and Si irradiated GaN epilayers

The as-deposited CdS thin films were irradiated with silicon ions at different fluences. The effects of Si ion irradiation on the structural and optical properties of CdS thin films were investigated. Metallic cadmium clusters or CdO were formed (XRD pattern) in irradiated films (1×10^{14} ions/cm²). The Raman peaks position of the as-deposited CdS film appears at 299 cm⁻¹ due to scattering from CdS (LO) mode. The peak position remains constant and the FWHM increased at high fluences of Si ion [3]. For photoluminescence (PL) measurements, a He-Cd laser is employed as the excitation source, the CdS thin films exhibits a luminescence peak near band-edge at 2.54eV which may be attributed to bound excitons. Similarly the Si ion irradiated ZnSe thin films were also characterized. Detailed study is in progress.

REFERENCES

- [1] Y.C. Chang, A.E. Oberhofer, J.F. Muth, M. Kolbas, and R.F. Davis, Appl. Phys. Lett. 79 (2001) 281

- [2] S.O. Kucheyev, J.S. Williams, S.J. Pearton, Mater. Sci. and Eng.B. 33 (2001) 51.
 [3] K.L. Narayanan, K.P. Vijayakumar, K.G.M. Nair, R. Kesavamoorthy, Nucl. Instr. and Meth. in Phys. Res. B 160 (2000) 471

5.2.13 Effect of 190 MeV Ag ion irradiation on magnetization of NiMn_{0.05}Ti_{0.2}Mg_{0.2}Fe_{1.55}O₄ ferrite thin film

Anjana Dogra^{1,4}, Ravi Kumar⁴, V. V. Siva Kumar⁴, D. C. Kundaliya², S. K. Malik², N. Kumar³ and M. Singh¹

¹H.P University, Summer Hill, Shimla-171 005

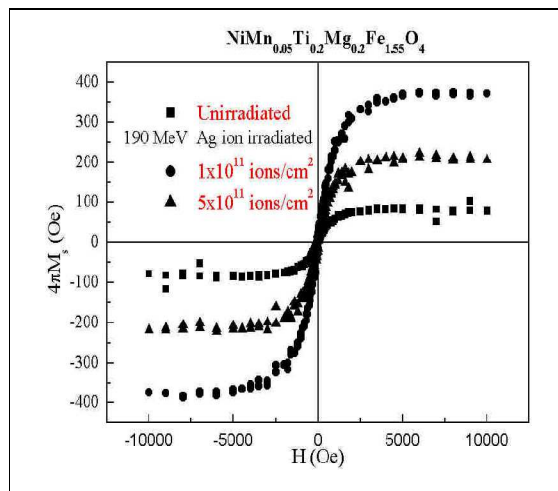
²Tata Institute of Fundamental Research, Mumbai-400 005

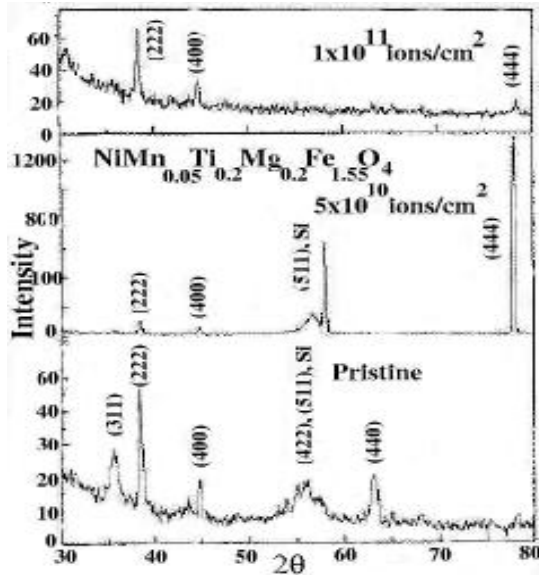
³Solid State Physics Laboratory, Timarpur, New Delhi-110 054

⁴Nuclear Science Centre, New Delhi-110 067

Irradiation studies on the ferrite thin film will help to enhance the understanding the magnetic properties of ferrite systems. Here we present the fluence dependence effect of 190 MeV Ag ion irradiation on NiMn_{0.05}Ti_{0.2}Mg_{0.2}Fe_{1.55}O₄ ferrite thin film. Bulk target of NiMn_{0.05}Ti_{0.2}Mg_{0.2}Fe_{1.55}O₄ was synthesized by ceramic route. Thin film on Si<100> substrate from same target was deposited by rf magnetron sputtering. Prepared thin films were irradiated with 190 MeV Ag ion in the fluence range 5x10¹⁰ - 1x10¹² ions/cm² using 15UD Pelletron at Nuclear Science Centre, New Delhi. For the structural analysis of the unirradiated and irradiated films X-ray diffraction (XRD) was performed using Philips Diffractometer PW 3020 CuKα. The DC magnetization measurements at room temperature on the unirradiated and irradiated films were carried out using Quantum design SQUID magnetometer. XRD for the structural analysis confirms the cubic structure of the films. From the XRD pattern shown in figure 1 it is observed that the pristine film shows all the spinel peaks. Whereas in the irradiated films the dominance of <222> and <444> is noticed which suggest the defect induced texturing of the films along the <111>, an easy axis of magnetization in spinel ferrites. With the increase in the fluence, the background in the films increases which can be correlated to the amorphization of the films on irradiation.

Fig. 1 XRD patterns of the pristine and 190 MeV Ag ion irradiated films NiMn_{0.05}Ti_{0.2}Mg_{0.2}Fe_{1.55}O₄





The magnetization values calculated from the hysteresis show an increase upto the fluence of 1×10^{11} ions/cm². After this fluence, value the magnetization show a decrease. It is also noticed that all the irradiated films show larger magnetization value than the unirradiated film. The increase in the magnetization can be expected due to the texturing of the films along an easy axis observed in the XRD pattern. This observation implies that the alignment of the magnetic moment with the application of magnetic field is much easier in the irradiated textured films which results in the increase in the magnetization. After the fluence of 1×10^{11} ions/cm², the intensity of the $\langle 222 \rangle$ and $\langle 444 \rangle$ peak decreases and also the broadening of these peaks is being observed which thereby decrease the magnetization. This decrease in the magnetization value can be correlated to the amorphization of the films after certain fluence.

5.2.14 Effect of 50 MeV Li³⁺ Ion Irradiation on Dielectric Properties of Erbium Orthoferrite Single Crystals

K.K.Bamzai¹, Monita Bhat¹, Balwinder Kaur¹, P.N.Kotru¹, B.M.Wanklyn² and Ravi Kumar³.

¹Crystal Growth and Materials Research Group, Dept. of Physics & Electronics, University of Jammu, Jammu – 180006.

²Dept. of Physics, Clarendon Laboratory, University of Oxford, Oxford OX1 PU, U.K.

³Nuclear Science Centre, New Delhi – 110067

Orthoferrites have the general formula REFO₃ where R is a large trivalent metal ion, such as a rare earth or an Y ion. They crystallize in a distorted perovskite structure with an orthorhombic unit cell [1]. These ferrites are highly suitable for use in memory and switching circuit of digital computer [2,3]. Irradiation induced modification of a ma-

terial is a current subject of interest for the researcher and is at present a widely studied subject to understand the damage structures and the modifications on their physical properties [4-5]. In the present study, we investigated the dielectric properties of the system of Erbium Orthoferrites before and after irradiation.

ErFeO₃ crystals were grown by flux growth technique [6]. The dielectric constant was determined before and after irradiating the crystals, using a (HP 4192A LF) fully automated Impedance Analyzer. For irradiation, we use 50MeV Lithium Ion Beam (Li³⁺) with fluence 5x10¹³ ions/cm² at NSC, New Delhi.

The variations of dielectric constant ϵ' for ErFeO₃ single crystals was studied as a function of an applied a.c. field in the frequency range from 1kHz to 10MHz in the temperature range of 30-550°C. Fig.1 shows the dielectric constant as a function of frequency for unirradiated as well as irradiated ErFeO₃ crystals. At each particular temperature ranging from 30-550°C the dielectric constant shows decrease in its value as the frequency is increased and becomes almost saturated beyond 100kHz. This decrease in the behaviour of dielectric constant with increasing frequency is normal behaviour of

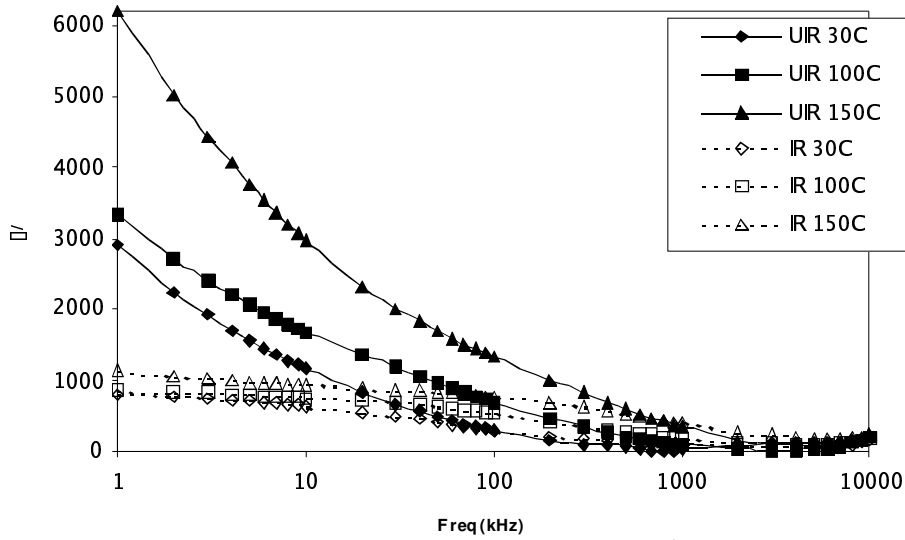


FIGURE 1 Plot showing the variation of dielectric constant (ϵ') with frequency for unirradiated and irradiated ErFeO₃ at various temperatures.

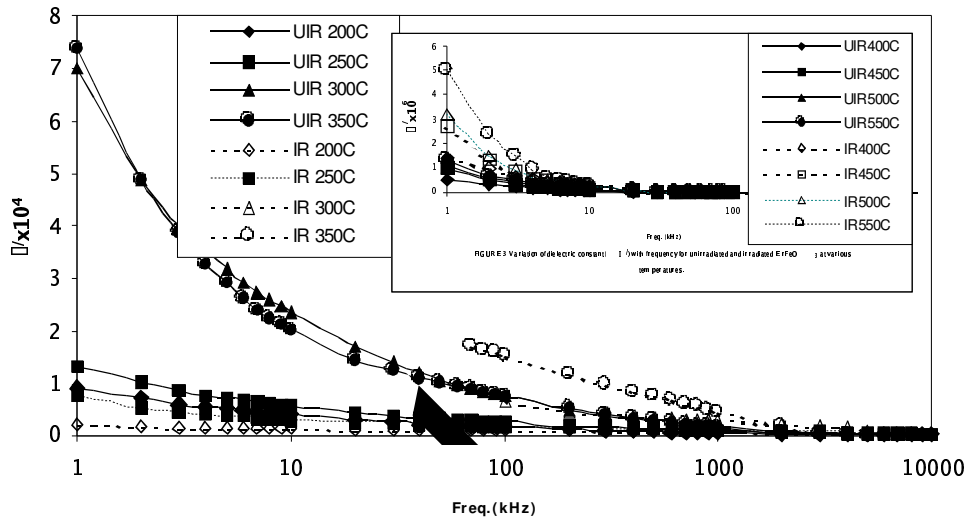


FIGURE 2 Plot showing the variation of dielectric constant (ϵ') with frequency for unirradiated and irradiated ErFeO_3 at various temperatures.

ferrites and is consistent with the Koops model [7]. After irradiation, at each particular frequency the value of dielectric constant decreases in the temperature range of 30-300°C. This decrease in ϵ' may be due to the decrease in space charge carriers or interfacial polarization in irradiated sample [8]. At 300°C the values of ϵ' for both irradiated and unirradiated become almost same whereas above 300°C, the magnitude of ϵ' increases for the irradiated samples as compared to the unirradiated samples. This behaviour can be explained on the basis that the mechanism of polarization process in ferrites is similar to that of conduction process. The electronic exchange between Fe ions gives local displacement of electrons in the direction of an applied electric field, which induces polarization in ferrites. The anomaly in the variation of dielectric constant after irradiation is due to the defect creation [9], which results in a collective contribution of p and n type conduction. It is well known that the local displacement of the p-type carriers take part in the polarization in an opposite direction to that of the external field [10]. In addition since the mobility of p type carrier is lower than that of n type carrier, their contribution to polarization decreases more rapidly at lower temperatures thereby reducing the value of ϵ' in the case of irradiated samples. After irradiation below 300°C there is n type conduction and beyond this there is collective contribution of both n and p type carriers.

REFERENCES

- [1] C.Rao, Solid State Chemistry. Marcel Dekker Inc. (1974) p.29, 30, 32, 33, 357, 394.
- [2] W.N.Papian, Proc. Metal Powder Assoc. Lond. **2**, (1955).
- [3] Carl Heck. "Magnetic Materials and their applications" (Butterworth, London, 1974).
- [4] J.M.Costantini, F.Studer, J.C.Penzin, J.Appl. Phys. **90** (2001) 126.
- [5] S.Furuno, N.Sasajima, K.Hojou, K.Izui, H.Otsu, T.Muromura, T.Matsui, Nucl. Instr and Meth.B **127/128** (1997) 181.

- [6] B.M.Wanklyn, J.Cryst Growth, **5** (1969) 323.
 [7] C.G.Koops, Phys. Rev. **83**, (1951) 121.
 [8] M.A.Madare, S.V. salvi, Ind. J.Phys. **75A** (2001) 363.
 [9] J.Provost et.al, Materials Research Society, (1995) 22.
 [10] A.N.Patil et.al, Bull. Mater. Sci. **23** (2000) 447.

5.2.15 Irradiation Effects on Mechanical Behaviour of Pure & Substituted M – type Strontium Hexaferrite and Orthoferrite Single Crystals.

K.K.Bamzai¹, Balwinder Kaur¹, Monita Bhat¹, P.N.Kotru¹, F. Licci², B.M.Wanklyn³ and Ravi Kumar⁴.

¹Crystal Growth and Materials Research Group, Department of Physics and Electronics, University of Jammu, Jammu – 180006.

²Instituto MASPEC – CNR, Via Chiavari 18/A, 43100 Parma, Italy.

³Dept. of Physics, Clarendon Laboratory, University of Oxford, Oxford OX1 3PU, UK.

⁴Nuclear Science Centre, New Delhi – 110067.

Hexaferrites with the magnetoplumbite or related structures are the most promising materials because of their strong magnetic anisotropy [1-2] whereas rare earth orthoferrite find applications in communication technique, in sensors of magnetic fields etc. The hardness of ferrites with respect to breakage depends upon its resistance to the expansion of cracks and so the study on propagation of cracks is of great significance. Among the properties of materials that affect microhardness, the main ones are its growth/ preparation, chemical inhomogeneity, defects and so on. All these factors are reduced greatly in case of a single crystal grain under controlled conditions.

Swift Heavy Ions can produce additional defects, create phase transformations and give rise to anisotropic growth to some materials. In the present case, pure and substituted Strontium hexaferrite and rare earth orthoferrite REFeO₃ (where R=Gd, Er, Y) were irradiated with 50 MeV Li³⁺ ion with different fluence ranging from 1x10¹², 1x10¹³, 5x10¹³ and 1x10¹⁴ ions/cm² using 15UD Pelletron Accelerator at Nuclear Science centre, New Delhi. Mechanical behaviour of these materials was studied before and after irradiation. Fig.1 shows graph of Vicker's microhardness with load for pure SrFe₁₂O₁₉ and substituted Ga-In of the form SrGa_xIn_yFe_{12-(x+y)}O₁₉ (where x = 5, 7, 9 and y = 0.8, 1.3, 1). This non-linear behaviour of microhardness with applied load is also true in case of Rare earth orthoferrite. Fig.1 clearly shows decrease in the value of microhardness for irradiated samples and this decrease is attributed to the certain types of amorphization and presence of deep cracks. It is clear from the figure that microhardness value decreases non-linearly with the increase in load upto a certain value and thereafter it attains saturation. Hays and Kendall's law explains this type of non-linear behaviour, which is a modification of Kick's law [3-4]. It is also clear that Vickers microhardness increases with substitution and is maximum for highly substituted Sr- hexaferrite. Fig.2 shows the linear increase in crack length with ap-

plied load. The crack length increases after irradiation, which is further substantiated from photomicrograph as shown in Fig.3 (a,b).

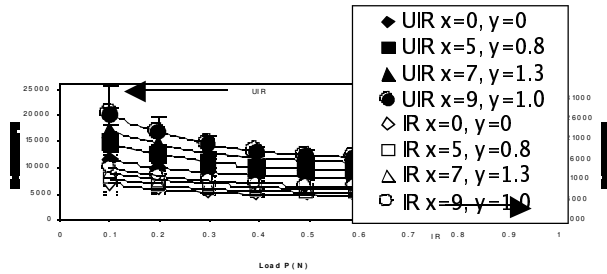


Fig.1 Plot showing the Vickers hardness vs. Applied load for un-irradiated and irradiated polymer and GeH₄ irradiated SPe. 11 011

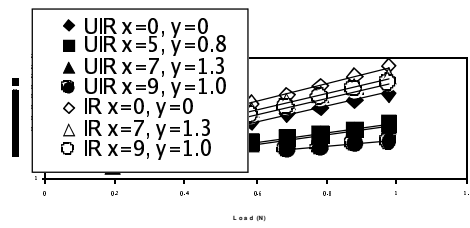


Fig.2 A curve showing the effect of load on crack length for un-irradiated and irradiated polymer and GeH₄ irradiated SPe. 11 011

Fig.1:



Fig. 3(a)

Fig.2:

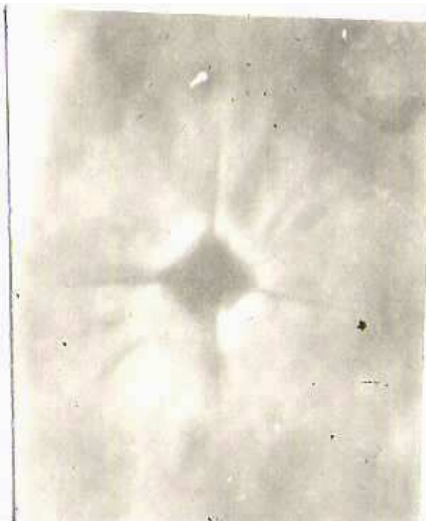


Fig. 3(b)

Fig. 3(a) Indentation mark taken before sample is taken for irradiation.

Fig. 3(b) Indentation mark taken after the sample is irradiated clearly showing the development of cracks.

REFERENCES

- [1] J. Nicolas, "Microwave Ferrites" in Ferromagnetic Materials" Ed. E. P. Wohlfarth, North Holland, Amsterdam (1980).
- [2] A. H. Eschenfelder, "Magnetic Bubble Technology", Springer Verlag, Berlin (1980)
- [3] C. Hays, E.G. Kendall, Metallography 6 (1973) 275.
- [4] F. Kick, Das gesetz der, Proportionalen Widerstande and Siene Anwendung, Delipzig Felix 1885.

5.2.16 Irradiation Effects on Dielectric Behaviour of M – type Strontium Hexaferrite Crystals.

K.K.Bamzai¹, Balwinder Kaur¹, Monita Bhat¹, P.N.Kotru¹, F. Licci² and Ravi Kumar³

¹Crystal Growth and Materials Research Group, Dept. of Physics & Electronics, University of Jammu, Jammu – 180006.

²Instituto MASPEC – CNR, Via Chiavari 18/A, 43100 Parma, Italy.

³Nuclear Science Centre, New Delhi - 110067.

The dielectric properties of ferrites depend upon factors namely chemical composition, method of preparation, grain size etc. Study of dielectric properties means the behaviour of a material to an electric field. Swift Heavy Ions irradiation provides several interesting aspects in understanding damage structure and material modifications. The effect of energetic ion beam with material depends on the ion energy, fluence and ion species. The ions either excite or ionize the atoms by inelastic collisions or displace atoms by elastic collisions. It is evident that electronic energy loss, S_e , due to inelastic collision is able to generate point/ cluster of defects if S_e is less than the threshold value of electronic energy loss (S_{eth}) [1-2]. If S_e is greater than S_{eth} , then the energetic ions can create columnar amorphization.

The samples were irradiated with 50 MeV Li^{3+} ion using 15 UD Pelletron facility at Nuclear Science Centre, New Delhi at different fluences of 1×10^{12} , 1×10^{13} , 5×10^{13} , and 1×10^{14} ions/cm². In the present study, the dielectric behaviour of unirradiated and irradiated single crystals of pure Strontium hexaferrite ($SrFe_{12}O_{19}$) at 1×10^{13} ions/cm² are discussed. The dielectric measurements as a function of frequency can provide understanding of the material modification due to created defects by irradiation.

The variation of dielectric constant (ϵ') and dielectric loss ($\tan\delta$) with frequency in the temperature range (20 – 200°C) is shown in Figs. 1 and 2. It is noted that ϵ' increases at every temperature after irradiation. The dielectric constant decreases with increase in frequency, which is the normal behaviour of ferrites and can be explained by Koop's phenomenological theory [3]. The peaks in the loss factor can be explained on the basis of relative variation of ϵ' and ϵ'' with frequency [4]. The peaks in $\tan\delta$ can be attributed to the Maxwell – Wagner Interfacial Polarization i.e., matching of hopping frequency with

frequency of external electric field [5-6]. Fig. 3 shows the temperature dependence of dielectric constant at different frequencies of applied a.c. field. There is almost a linear rise in ϵ' at all frequencies of unirradiated and irradiated crystals. Fig. 4 shows dependence of conductivity on temperature at different frequencies, which increases with increase in temperature.

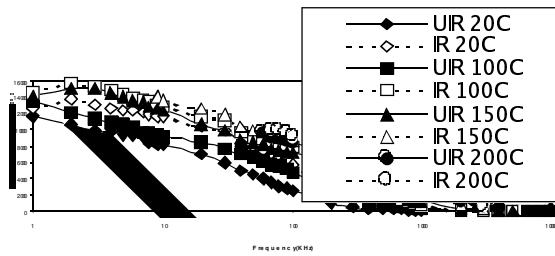


FIGURE 1 Plot showing the frequency dependence of ϵ' at different temperatures for unirradiated and irradiated SrFeO₃.

Fig. 1:

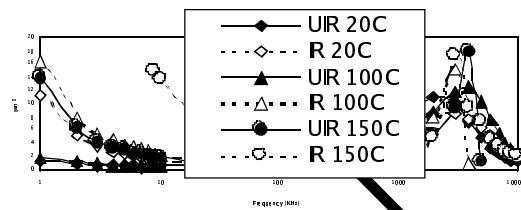


FIGURE 2 Plot showing the variation of $\tan \delta$ with frequency at various temperatures for unirradiated and irradiated SrFeO₃.

Fig. 2:

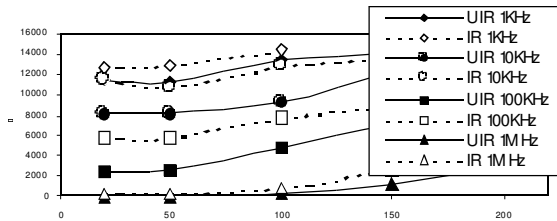


FIGURE 3 Graph showing the variation of ϵ' with temperature at various frequencies for unirradiated and irradiated SrFeO₃.

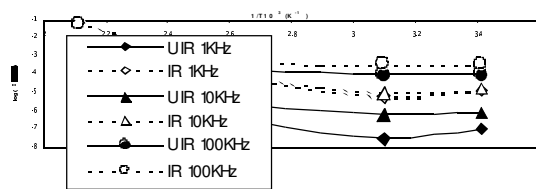


FIGURE 4 Graph showing the variation of a.c. conductivity (σ) with temperature at various frequencies for unirradiated and irradiated SrFeO₃.

Fig. 3:**Fig. 4:****REFERENCES**

- [1] M. Toulmonde, Nucl. Instr. and Meth. B 156 (1999) 1.
- [2] G. Szenes, Phys. Rev. B 51 (13) (1995) 8026.
- [3] C. G. Koop's Phys. Rev. 83 (1951) 121.
- [4] L. G. Van, Uitert, Proc. I. R. E. 44 (1956) 1294.
- [5] J. C. Maxwell A Treatise in electricity and magnetism (New York: Oxford University Press) Vol. 2 (1954).
- [6] K. W. Wagner Amer. Phys. 40 (1913) 817.

5.2.17 Structural and Optical Modifications of LiF Thin Films

M. Kumar¹, F. Singh⁵, S. A. Khan⁵, V. Baranwal¹, S. Kumar³, D. Agarwal³, A. M. Siddiqui^{5,4}, A. Tripathi⁵, A. Gupta², D. K. Avasthi⁵ and A. C. Pandey¹

¹Department of Physics, University of Allahabad, Allahabad-211 002

²IUC-DAEF, University Campus, Khandwa road, Indore, 452 017

³Department of Physics, R. B. S. College, Agra-282 002

⁴Department of Physics, Jamia Millia Islamia, Jamia Nagar, New Delhi - 110 025

⁵Nuclear Science Centre, New Delhi-110067

The LiF thin films, thermally deposited on glass substrate, were irradiated by 150 MeV Ag⁹⁺ ions under high vacuum with different ion fluences using 15UD Pelletron at Nuclear Science Centre, New Delhi. The fluence was varied from 5×10^{11} to 7×10^{12} ions/cm². The SHI induced structural and optical modifications were studied using glancing angle X-ray diffraction (GAXRD), optical absorption spectroscopy and photoluminescence (PL).

For structural analysis, GAXRD studies were performed on pristine and irradiated films using Siemen diffractometer D5000 with CuK_a (1.54056 Å) in the 2θ range 30-80° with step size of 0.05°. GAXRD result on deposited thin films of LiF shows that films are polycrystalline in nature dominated by (111) plane. Pristine and irradiated films show peaks along (111), (200), and (220) as shown in the inset of Figure 1. The average grain size of these films were calculated from the FWHM of (111) peak using Scherrer formula. The grain size decreases from 46.2 nm (for pristine) to 18.3 nm (for 3×10^{12} ions/cm² fluence) followed by some increase (Fig.1). This reduction is attributed to strain induced fragmentation of grains. According to thermal spike model, the energy is deposited by the projectile on the electronic subsystem of the target. Then this energy is shared between the electrons by electron-electron coupling. This energy is transferred to the lattice atoms by the electron-lattice interaction (i.e. electron-phonon coupling) leading to a large increase in temperature along the ion path. Due to the temperature spike there will

be development of pressure which will cause the strain in the grain. This strain leads to fragmentation of grains. As the fluence increases the energy transferred by ions to the electronic subsystem will increase which result in the further decrease in the grain size.

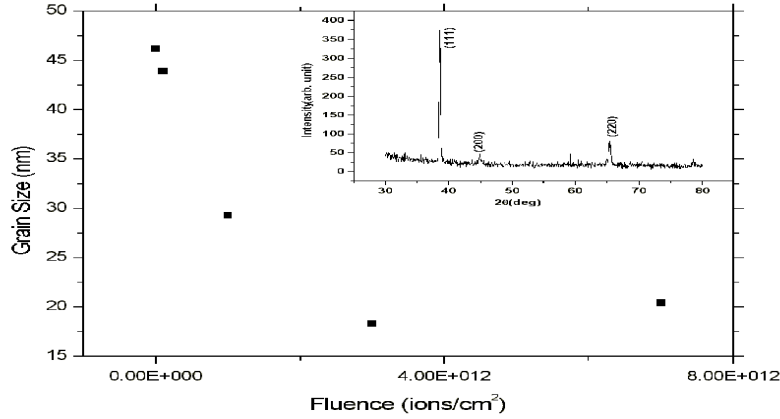
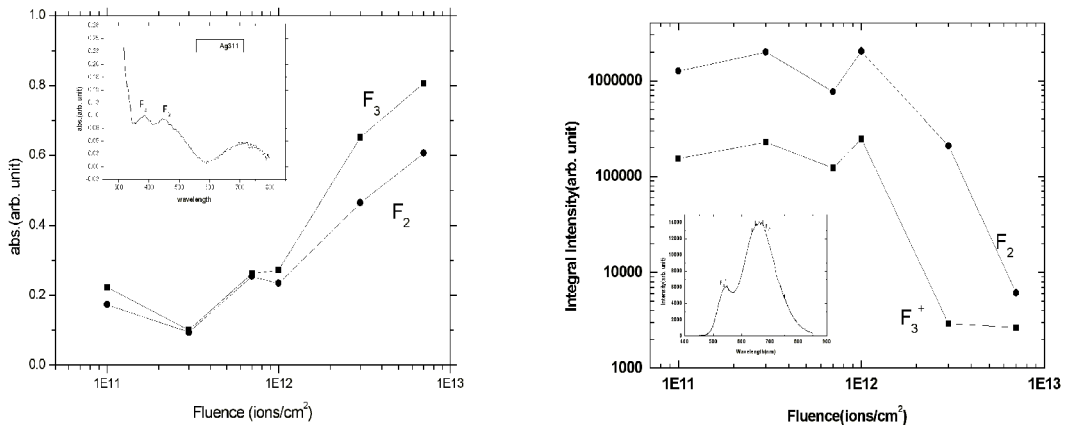


Fig 1: Grain size variation with fluence, the inset in the figure is the GAXRD spectra of pristine sample.

Optical absorption studies showed the absorption band peaked at a wavelength 380 and 445 nm corresponding to F_3 and F_2 color centers respectively [1, 2, 3]. The inset of Figure 2(a) shows primary absorption spectrum. It is observed that the absorbance increases with ion fluence for both the color centers as shown in the Figure 2(a). From Smakula-Dexture formula [2], we can evaluate the concentration of F_2 -centers. The number of F_2 centers increases with fluence. RT photoluminescence spectra of SHI irradiated samples shows two broad bands peaked at about 534 and 665 nm corresponding to F_3^+ and F_2 color centers respectively [1,4,5]. The observed spectra at different ion fluences were fitted using two



Gaussian peaks. Figure 2(b) shows the variation of the integral intensity of these two bands. The intensity of both bands remains almost constant up to fluence of 1×10^{12} ions/cm² followed by drastic decrease. The peak intensity is sensitive to damage. Initially strong integrated PL intensity indicate dominant radiative relaxation transitions. In the

presence of near-surface damage layer, the non-radiative relaxation transition rate will increase, thus decreasing the integrated PL intensity from the sample.

(a)

(b)

Fig. 2(a): Variation of absorbance with ion fluence. The inset in the Figure is the absorption spectra for 3×10^{11} ions/cm² fluence irradiated sample.

Fig. 2(b): Integral intensity variation of F_3^+ and F_2 color centers. Inset in the Figure presents the primary PL spectra of irradiated sample.

REFERENCES

- [1] F. Singh et al., Radiation Measurement 36, 675 (2003)
- [2] K. Schwartz et al., Phys. Rev. **B58**, 11232 (1998).
- [3] G. Baldacchini et al., Thin Solid Films **330**, 67 (1998).
- [4] R. M. Montereali et al., Thin Solid Films **205**, 106 (1991).
- [5] M. Kumar et al., NSC Annual Report, 230, 2002-2003.

5.2.18 Photoluminescence Studies in Swift Heavy Ion Induced Mullite

B. N. Lakshminarasappa ¹, H. Nagabhushana ¹, Fouran Singh ² and D.K. Avasthi ²

¹Department of Physics, Bangalore University, Bangalore – 560056

²Nuclear Science Centre, New Delhi – 110067

Aluminum silicate (Al_2SiO_5) polymorphs are promising materials for high temperature applications because of its low thermal conductivity. The binary system of Al_2SiO_5 contains four naturally occurring compounds, three of them-kyanite, sillimanite and andalusite have the composition $Al_2O_3 \cdot SiO_2$ and the fourth one is mullite having the composition $3Al_2O_3 \cdot 2SiO_2$ occurs rarely in natural rocks and crystallizes in orthorhombic. The silicate group is used in the production of non-fusion cast tanks, in the manufacture of spark plugs and as a mineral specimen. Nano size particles of mullite have been synthesized by solution combustion (I) and sol-gel (II) techniques [1,2]. Here, we report the photoluminescence (PL) behavior of synthetic aluminum silicates bombarded with 100 MeV Swift heavy Ni^{+8} followed by laser excitation.

Mullite pellets of 1 mm thickness and 6 mm diameter are prepared using an home made palletizer. The pellets of these samples are bombarded with 100 MeV Ni⁸⁺ ions with fluence in the range from 10¹¹ to 10¹⁴ ions/cm² at Nuclear Science Centre. For in-situ PL measurements, a Kimmon He-Cd laser through a sapphire window is used. A mirror to make the laser incident on a sample kept in vacuum chamber deflects laser beam. A vacuum-sealed optical sapphire window is provided in a chamber for collection of fluorescent light. The entry of the laser beam from the ground level is the same so that the effect of ion irradiation in the sample can be studied by simply switching the beam on and off.

Photoluminescence of mullite sample I and II irradiated with 100 MeV Ni⁺⁸ ions for fluences in the range 1×10¹¹-1×10¹⁴ ions/cm², excited by 442 nm laser beam excitation are recorded. A broad emission band with peak at ~557 nm besides a sharp emission band with peak at 705 nm is observed in sample I. However, a single emission band with peak at about 537 nm is recorded in sample II. The PL intensity in both samples I and II are found to decrease with increase of ion fluence. This may be attributed to irradiation-induced amorphization as a result of cascade quenching [3,4]. Amorphization may take place in the system as each incident ion may create one or several displacement cascades, which become amorphous as a result of rapid quenching, and these cascades eventually overlap to form an amorphous solid [3]. The susceptibility of amorphization may be measured in two ways: (i) the ion dose required for amorphization at a fixed irradiation temperature or (ii) the critical temperature. Wang et al. [3] have observed the complete amorphization in Al₂SiO₅ by monitoring the selected area diffraction technique (SAD) under 1.5 MeV Xe⁺ ions with the fluence of 1.8×10¹⁴ ions/cm², and the critical temperature for amorphization of kyanite was observed to be 1281 K. It is also found that the PL intensity in sample I is more compared to that in sample II. This is attributed to the physical nature of the sample, preparation conditions and/or ingredients used in the preparation of phosphor.

The infrared absorption of pristine and that of ion irradiated mullite (I and II) with a fluence of 1×10¹³ ions/cm² have been studied. The spectra revealed the characteristic absorption bands of silicates and water before irradiation of the samples. It is observed that the sharpness of the peaks is high in SHI irradiated samples. This could be attributed to close packing of the molecules or to confirmation changes in the molecules or both [5]. The decrease in the PL intensity in both the samples might be due to the destruction of Si-O and Al-O bonds. And, the destruction of these bonds with irradiation may further enhance the amorphous nature of the sample. The irradiation effects may lead to the restructuring of the surface chemical species because of the energy deposited through electronic loss during the process of swift heavy ion irradiation and, formation of ion induced defects leading to non-radiative recombination centers. These two processes are simultaneous and they compete with each other. Consequently, the enhancement or degradation of PL might be due to the balance between these two effects [6].

REFERENCES

- [1] R.G. Chandran, K.C. Patil, G.T. Chandrappa, Int. J. Self-Propag. High-Temp. Synth. 3 (1994) 13

- [2] P. Brovetto, A. Delunas, V. Maxia, M. Salis, G. Spano, *Nuovo Cimento D* 13 (1991) 1379
- [3] E.S. Dana, E.M. Ford, *Minerology*, Asia Publishing House, Bombay, (1962) 617
- [4] T. Diaz de la Rubia, G.H. Gilmer, *Phy. Rev. Lett.* 74 (1995) 2507.
- [5] S. Narasimha Reddy, P.S. Rao, R.V.S.S.N. Ravikumar, B.J. Reddy, *Indian J. Phys.* 75A (2001) 429.
- [6] T.M. Bhave, S.S. Hulavarad, S.V. Bhoraskar, S.G. Hegde, D. Kanjilal, *Nucl. Instr. And Meth. B* 156 (1999) 121.

5.2.19 Lithium Ion Irradiation Effects in P(VDF-HFP) based Polymer Electrolytes

D. Saikia¹, A. M. P. Hussain¹, A. Kumar¹, F. Singh² and D. K. Avasthi²

¹Department of Physics, Tezpur University, Napaam, Tezpur, Assam-784028

²Nuclear Science Centre, New Delhi-110067

Swift Heavy Ion Irradiation in polymer electrolyte is the new area of research. In case of high energy ion irradiation of polymers, the electronic energy loss of the incident particle is released into (i) radiative decay (ii) production of new reactive species (radicals, gases) and defects (unsaturation, scissions, crosslinks) and heat and (iii) decrease in crystallinity has been reported after ion irradiation [1].

Both P(VDF-HFP)-(PC+DEC)-LiClO₄ and P(VDF-HFP)-LiClO₄ electrolyte samples were irradiated with swift heavy ion beam of Li³⁺ of energy 48 MeV with five different fluences (5×10^{10} , 10^{11} , 5×10^{11} , 10^{12} and 5×10^{12} ions/cm²). Ionic conductivities of both pristine and irradiated polymer electrolytes were evaluated from the complex impedance plots in the temperature range (303K to 343K) using a Hioki 3532-50 LCR Hitester in the frequency range 42 Hz to 5 MHz. Figure 1 shows conductivity versus temperature inverse plots of pristine and irradiated P(VDF-HFP)-(PC+DEC)-LiClO₄ polymer electrolyte systems. Figure shows that the ionic conductivity increases after irradiation with fluences upto 10^{11} ions/cm² and at still higher dose the conductivity decreases [2].

X-ray diffractograms have been taken by Phillips X'pert Pro diffractometer in the range of 2θ from 3° to 100°. Figures 2 and 3 show the X-ray diffractograms of pristine and irradiated P(VDF-HFP)-LiClO₄-(PC+DEC) and P(VDF-HFP)-LiClO₄ polymer electrolyte systems respectively. XRD pattern show decrease in crystallinity of polymer electrolytes after irradiation at low fluence ($\leq 10^{11}$ ions/cm²), whereas at higher fluence amorphicity decreases. XRD results corroborate the ionic conductivity results. At low fluences ($\leq 10^{11}$ ions/cm²) amorphicity increases giving rise to increase in ionic conductivity and at high fluences amorphicity decreases resulting in decrease in the conductivity [3]. Decrease in amorphicity at higher fluence could be attributed to the fact that at higher fluence activation energy barrier for crystallization is overcome and degree of crystallinity of the polymer electrolyte increases.

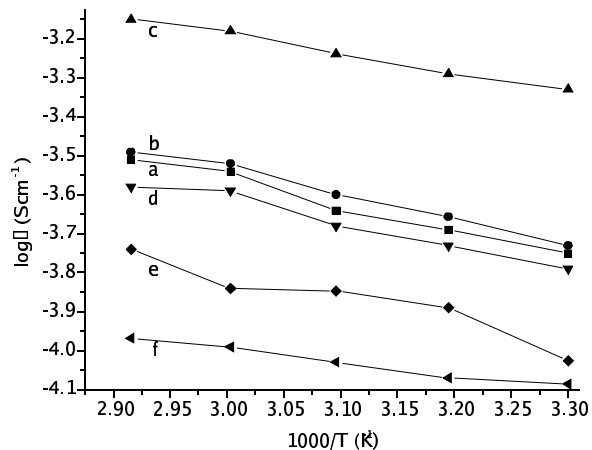


Fig.1: Temperature dependence of ionic conductivity of P(VDF-HFP)-(PC+DEC)-LiClO₄ gel polymer electrolyte (a) pristine, (b) 5×10^{10} , (c) 10^{11} , (d) 5×10^{11} , (e) 10^{12} and (f) 5×10^{12} ions/cm²

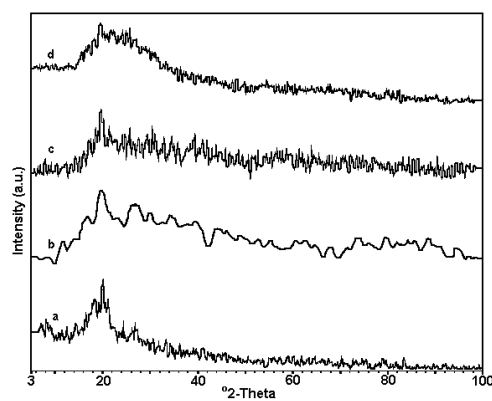


Fig. 2: XRD Spectra of (a) P(VDF-HFP), (b) P(VDF-HFP)-(PC+DEC)-LiClO₄, (c) Li ion irradiated P(VDF-HFP)-(PC+DEC)-LiClO₄ [5×10^{10} ions/cm²], (d) Li ion irradiated P(VDF-HFP)-(PC+DEC)-LiClO₄ [5×10^{12} ions/cm²]

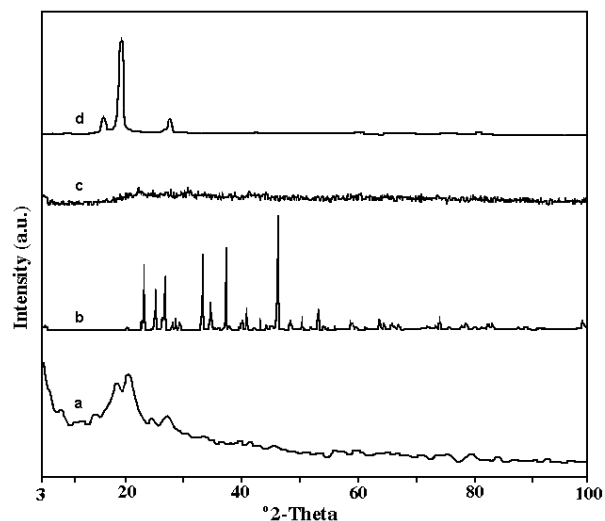


Fig. 3: XRD Spectra of (a) P(VDF-HFP), (b) LiClO₄, (c) Unirradiated P(VDF-HFP)-LiClO₄ (d) Li ion irradiated P(VDF-HFP)- LiClO₄ [5×10^{12} ions/cm²]

From the scanning electron micrographs of pristine and irradiated P(VDF-HFP)-(PC+DEC)-LiClO₄ and P(VDF-HFP)-LiClO₄ polymer electrolyte systems, it is observed that electrolyte films are two phase system having polymer and liquid electrolyte phases. Here the film is interspersed with pores filled with liquid electrolyte, which form a connected path through the polymer matrix [4]. After ion irradiation of the polymer electrolyte systems porosity increases. Increased porosity results in the enhancement of ionic conductivity in polymer electrolytes.

REFERENCES

- [1] V. Chailley, E. Balanzat and E. Dooryhee, *Nuclear Instruments and Physics Research B*, 105 (1995) 110.
- [2] H. Wang, H. Huang and S. L. Wunder, *J. Electrochem. Soc.* 147(8) (2000) 2853.
- [3] S. Panero, D. Satolli, A. D'Epifano and B. Scrosati, *J. Electrochem Soc.* 149(4) (2002) A414.
- [4] R A Zoppi and M C Goncalves, *Solid State Ionics* 147 (2002) 157.

5.2.20 Response Characteristics of OHP-films as Nuclear Track Detectors for Low Energy ¹⁶O Ions

B. Basu¹, S. Ghosh¹, A. Mazumdar^{1,2}, S. Raha¹, S. Saha³, Swapan K. Saha¹, Asiti Sarma⁵ and D. Syam⁴

¹Bose Institute, 93/1 A.P.C. Road, Kolkata-700009

²F.B. Physik, University of Marburg, Marburg, Germany

³Saha Institute of Nuclear Physics, Bidhannagar, Kolkata-700064

⁴Physics Department, Presidency College, 86/1 College Street, Kolkata-700073

The central scientific objective of this experiment is to calibrate some polymer track detectors (namely, overhead projector films i.e. OHP films) which are suitable for large area cosmic ray exposures. It has been suggested in the literature [1] that strange quark matter (SQM), consisting of nearly equal numbers of up, down and strange quarks, represents the *true* ground state of strongly interacting matter. If this is correct, then there should occur stable lumps of SQM, which would behave as very heavy nuclei with a very abnormal charge-to-mass ratio ($Z/A \ll 1/2$). In some recent papers [2,3] it has been argued that under suitable conditions small strangelets having initial $A \sim 60$ and $Z \sim 2$, impinging on the top of the terrestrial atmosphere with $\beta \sim 0.6$, may grow to $A \sim 350$ and $Z \sim 14$ by the time it comes down to mountain altitudes $\sim 3-4$ km and be left with a $\beta < 0.01$. It has been estimated [3] that such objects would have a much lower flux ($5-10 \text{ m}^{-2}\text{year}^{-1}$) compared to the primary cosmic ray flux ($\sim 1000 \text{ cm}^{-2} \text{ sec}^{-1}$) consisting mainly of protons; thus a very large area of detectors, which should be insensitive to protons and other light particles, would need to be exposed for definitive detection of SQM in cosmic rays.

Some types of polymer films (e.g. Lexan and CR-39), constituting one class of Solid State Nuclear Track Detectors (SSNTD), have previously been used to detect cosmic rays. But CR-39 and Lexan are costly plastics; moreover, the sensitivity of CR-39 to light ions would be somewhat counter-productive for the present purpose as it would retain a huge low- Z background. Our intention is to explore the possibility of using OHP-films, which are both cheap and readily available, for the purpose of detecting heavy ions, particularly the strangelets. It was felt necessary to investigate the detection range and capability of the polyethylene terephthalate films, i.e. study its response characteristics or 'calibrate' it, using various ion beams of different energies, specifically ions having $Z \sim 6-26$ and $\beta \leq 0.1$ such as low energy ^{16}O ions. Only after 'calibration' work the OHP-films may be pressed into service as strangelet detectors.

The irradiation of the OHP films along with some CR-39 sheets, serving as SSNTD-standards, were carried out. The pelletron delivered an average current of about 8.5 nA, which was cut down in the LIBR-I beam line so that $\sim 60,000$ ions passed through the exit flange per second. A rotating target-holder arrangement which can hold 22 targets at a time, was fitted with neatly cut plastic sheets of various types and used repeatedly for irradiation. While rotating, each target, together with the conveyor belt, stopped automatically in front of the exit flange. A manually operated reset switch could set the system in motion again after any suitable interval of time. The distance between the target and exit flange could be varied which permitted us to expose the plastic sheets to ^{16}O ions of different energies, for the layer of air between the target and the exit flange degraded the energy of the ions. TRIM-based calculations indicated that the energy of the ions was 53.6 MeV just outside the exit flange and in air the range of the ions was 6.4 cm.

After irradiation, some of the OHP films were chemically etched with 6.25N NaOH solution, kept at 55°C , for 4 hours in the Radiation Biology laboratory of NSC, for

preliminary evaluation. Subsequent examinations under microscope revealed good quality etch-pits and the track density was found to be consistent with our expectations. Fig.1 is a photomicrograph of a portion of an etched OHP film which was subjected to normally incident ions. Oblique incidence should yield etch-pits with elliptical openings and this was found to be the case with plastic sheets exposed at a grazing angle of 35° . See Fig. 2.

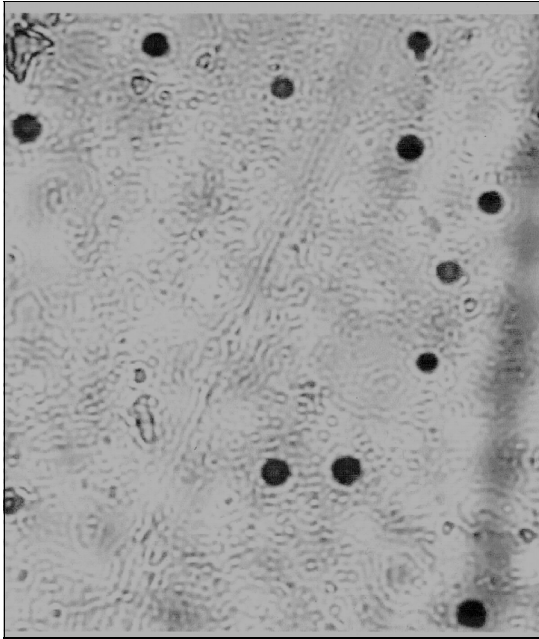


Fig. 1: Etch pits of ^{16}O for normal incidence

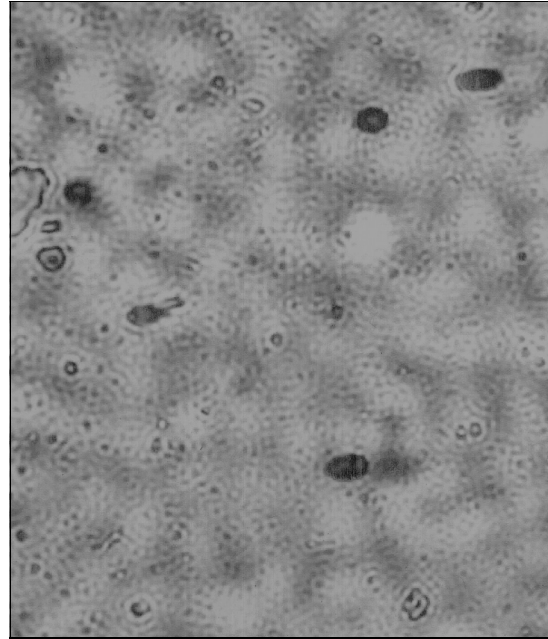


Fig. 2: Etch pits of ^{16}O for oblique incidence

REFERENCES

- [1] E. Witten, Phys. Rev. **D 30** (1984) 272
- [2] S. Banerjee, S. K. Ghosh, S. Raha and D. Syam, Phys. Rev. Lett. **85** (2000) 1384
- [3] S. Banerjee, S. K. Ghosh, A. Mazumdar, S. Raha and D. Syam, Astrophys. Space Sc. **274**_(2000) 655
- [4] S. Ghosh, J. Raju, P.P. Choubey and K. K. Dwivedi, Nucl. Tracks Radiat. Meas. **19** (1991) 77

5.2.21 Carbon-ion induced modifications in Poly (ethylene terephthalate): A free volume study

C. Ranganathaiah¹, Gani Shariff¹ and D. K. Avasthi²

¹Department of Studies in Physics, University of Mysore, Manasagangotri, Mysore -570 006

²Nuclear Science Center, New Delhi -110067

The free volume modifications in carbon-ion irradiated Poly (ethylene terephthalate) (PET) have been investigated using positron lifetime method. Ion beam irradiation is nowadays an established tool for modifying the structure and properties of polymers. Ion-beam irradiation induces dramatic chemical modifications in polymers [1]. The positron results indicate formation of linear tracks and free radicals on irradiation and iodine sorption suggests the filling of the free volume sites by iodine in the initial stages of sorption and in the later stages, swelling and conformational changes dominate. Generally, the lifetime spectra of most of the polymers are resolved into three (τ_1 , τ_2 and τ_3) lifetime components with respective intensities I_1 , I_2 and I_3 . The longest-living component τ_3 with intensity I_3 is due to pick-off annihilation in the free volume sites or low electron density regions present in the amorphous regions of the polymer matrix. The o-Ps lifetime τ_3 is the parameter of interest since a simple relation according to Nakanishi et al [2] relates it to the free volume hole size V_{f3} .

Utilizing the 15 MV Pelletron facility at Nuclear Science Center (NSC), New Delhi, carbon-ion irradiation of PET was carried out with a beam of 84 MeV $^{12}\text{C}^{6+}$ and fluence of 1×10^{12} ions/cm² and sorption of iodine was carried out by soaking this in 15-20 ml aqueous KI/Iodine solution. The PET samples were placed on either side of ^{22}Na positron source and placed between the two detectors of the Positron Lifetime Spectrometer (PLS) facility at DOS in Physics, University of Mysore, Manasagangotri, Mysore, to acquire lifetime spectrum. The data was analyzed into three lifetime components with the help of the computer program PATFIT-88 [3].

From the positron results of virgin and C-ion irradiated PET a sudden decrease in o-Ps lifetime τ_3 (1.76 to 1.65 ns), free volume V_{f3} (76.5 to 66 (Å³)) and o-Ps intensity I_3 (16.5 to 10.1%) for C-ion irradiated PET is observed compared to virgin PET. Ion-irradiation in polymers is known to produce breaking of atomic bonds in large numbers resulting in the formation of latent tracks [1]. These tracks will freeze and destroy some of the free volume holes along the ion path and result in a decrease of τ_3 and I_3 . During carbon-ion irradiation, PET molecules undergo chain scission. The decrease in lifetime and its intensity in C-ion irradiated PET compared to virgin PET is attributed to the formation of free radicals and thereafter cross linking of these radicals to form more stable radicals of the phenylene type.

Figure 1 shows the plot of τ_3 (V_{f3}) as a function of sorption time for C-ion irradiated PET. The changes in C-ion irradiated PET can be divided into two stages; the initial stage ($t = 380$ hrs) and final stage ($t > 380$ hrs). In the initial stage τ_3 remain a constant and then suddenly decreases suggesting the filling of the tracks (resulting from irradi-

ation) by iodine molecules. In the next stage τ_3 increase and a small decrease is observed thereafter. This can be attributed to the swelling of the polymer matrix and conformational changes respectively. In the final stage with $t > 380$ hrs τ_3 remains constant, suggesting that the filling of the free volume sites by iodine molecules is complete and iodine get precipitated.

Figure 2 shows a plot of (M_t / M_∞) versus $t^{1/2}$ for C-ion irradiated PET, which is generally called the sorption curve. M_t and M_∞ are the masses of the penetrant sorbed at times t and ∞ . The sorption curve is linear up to a value of approximately $(M_t / M_\infty) = 0.18$ and thereafter, the slope changes showing an upward curvature, suggests that the sorption is controlled by structural relaxation (swelling and conformational changes) of the polymer matrix in the presence of iodine.

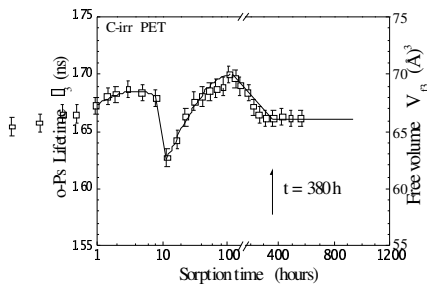


Figure 1: Variation of the o-Ps lifetime τ_3 and the free volume V_f as a function of sorption time for C-irr PET.

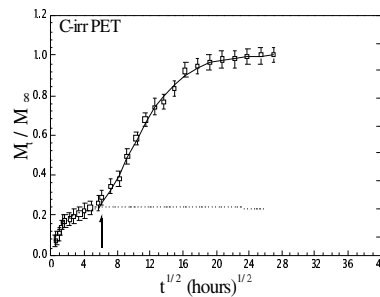


Figure 2: Variation of (M_t / M_∞) as a function of square root of sorption time for C-irr PET.

Fig. 1: Variation of the o-Ps lifetime τ_3 and the free volume V_f as a function of sorption time for C-irr PET

Fig. 2: Variation of (M_t / M_∞) as a function of square root of sorption time for C-irr PET

Using PLS technique, the modifications in PET upon carbon-ion irradiation are studied. The sudden decrease in τ_3 and I_3 in PET upon carbon-ion irradiation suggest that linear track formation results along the ion path and more cross links and stable free radicals are formed which leads to close packing of the polymer chains. Positron results on iodine sorption indicate filling of the free volume sites by iodine molecules accompanied by swelling and conformational changes.

REFERENCES

- [1] R. Percolla. L. Calcagno. G.Foti and G. Ciavola. Appl. Phys. Lett 65 (1994) 2966.
- [2] H. Nakanishi. S.J. Wang and Y.C. Jean. Positron Annihilation in Fluids Ed. by S.C. Sharma (World Scientific, Singapore 1988).
- [3] P. Kirkegaard. N.J. Pedersen and M. Eldrup. Report of Riso Natl. Lab., Denmark, M-2740 (1989).

5.2.22 Study of asymmetric membranes by gas permeation

Y.K.Vijay¹, N.K.Acharya¹, V.Kulshrestha¹, M. Singh¹, F.Singh² and D.K. Avasthi²

¹Department of Physics, University of Rajasthan, Jaipur-302 004

²Nuclear Science Center, New Delhi-110 067

In present work we aimed to prepare the asymmetric track etched polymer membranes. The polycarbonate membranes were of thickness of 18 μm , 25 μm and 38 μm and irradiated by Ni^{7+} ion of 100 MeV and subsequently etched in 6N NaOH at 60 °C. The ion fluence is of the order of $10^6, 10^7, 10^8$ ions/cm². These membranes were characterized by hydrogen and carbon dioxide gas permeation. For the same etching time these membranes have shown larger permeability from the irradiation side then the reverse side indicating the formation of conical tracks and asymmetrical membrane.

The distinctive properties of track etched membrane are a very narrow pore size distribution and a low sorption ability, which is especially important for the filtration of disperse systems. The irradiation of swift heavy ions in polymers changes the physical and chemical properties [1,2]. The passage of an energetic ion in polymers produces the latent tracks of reduced density and molecular weight. The track etch rate and bulk etch rate was measured at different etching temperature for Ar and Xe ion irradiated Makrofol-KL poly(carbonate) by Kumar et al. This shows that the etching temperature having an important role to determine the formation of the tracks [3].

When the range of an energetic ion is less than the thickness of the membrane then all the energy of incident ion beam losses in the material. Such membranes on etching the tracks, form asymmetric pores. However in case of transmitted tracks the track etching takes place from both the side of the membrane. The permeability of hydrogen and carbon dioxide increases with increasing etching time and at a particular etching time the drastic changes in permeability were observed as shown in Figure 1. The stopping range of Ni^{7+} ion of 100 MeV in polycarbonate is 22 μm . For 18 μm thick membrane, the etching time at which the permeability increases rapidly is less than that of 38 μm thick membrane for both the gases. In 38 μm thick and 10^8 ions/cm² irradiated membrane, it was observed 20 minutes and for 25 μm and same fluence it was 3 minutes.

The permeability from the ion incidence side (front) is more than that of ion emergence side (back) due to the shape of the track. So the polarity of the membrane is important for production of an asymmetric membrane [4]. The permeability of hydrogen is greater than that of carbon dioxide due the difference of their molecular sizes. The ion fluence also alters the permeation rates. The higher fluence membranes having less critical etching time than the lower fluence membranes. In case of 18m thick membrane, the critical etching time for 10^8 ions/cm² irradiated membrane was observed 1 minute whereas for 10^6 ions/cm² irradiated membrane it was observed 3 minutes.

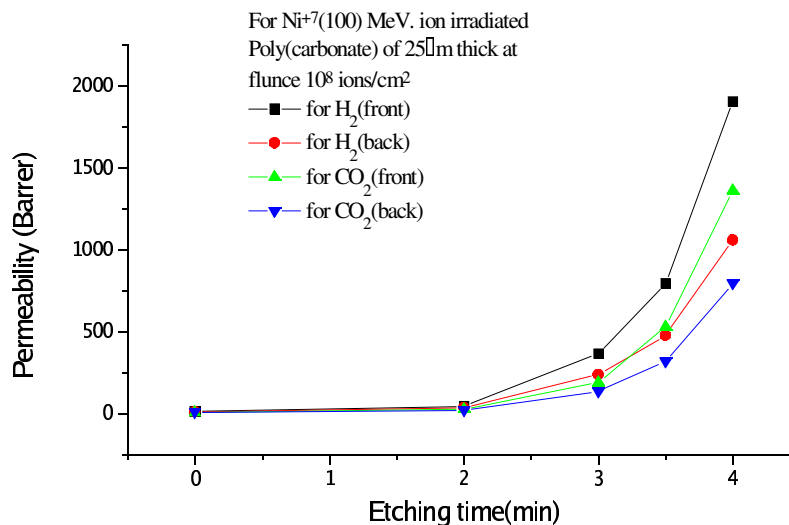


Fig. 1: Graph of permeability versus etching time

REFERENCES

- [1] C.Trautmann,S.Bouffard,R.Spohr, Nucl. Instr. and Meth. in Phys. Res. B 116 (1996) 429-433.
- [2] Y.K.Vijay, N.K.Acharya, S.Wate, D.K.Avasthi, Int. J. of Hydrogen Energy, 28 (2003) 1015-1018
- [3] Ashavani Kumar, Rajendra Prasad, Nucl. Instr. and Meth. in Phys. Res. B 168(2000) 411-416
- [4] P. Yu.Apel,Yu.E.Korchev,Z.Siwu,R.Spohr,M.Yoshida, Nucl. Instr. and Meth. in Phys. Res. B 184 (2001) 337-346

5.2.23 Energy loss and straggling measurements of light ions in different polymeric absorber foils

P.K. Diwan¹, V. Sharma¹, S. Kumar¹, S.K. Sharma², V.K. Mittal³, B. Sannakki⁴, R.D. Mathad⁴, S.A. Khan⁵ and D.K.Avasthi⁵

¹Department of Physics, Kurukshethra University, Kurukshethra

²Department of Phycis, Ambala College of Engineering and Applied Research, Ambala

³Department of Physics, Punjabi University, Patiala

⁴Department of Physics, Gulbarga University, Gulbarga

⁵Nuclear Science Centre, New Delhi-110067

The energy loss and straggling of Li(23, 30, 40 MeV) and C(40, 60, 80 MeV) ions in different polymeric foils viz. Polypropylene (C₃H₆), Polycarbonate(C₁₆H₁₄O₃), Mylar(C₁₀H₈O₄), Kapton(C₂₂H₁₀O₅N₂), LR-115(C₆H₉O₉N₂) have been measured. These measurements have been carried out utilizing low flux chamber, fixed with General Purpose Scattering Chamber (GPSC), at an angle of 15° with respect to the primary beam direction. The experimental arrangement is such that both the "unabsorbed" and

"absorbed" spectra through varying thicknesses of the absorber foils, for a particular ion at fixed energy, have been recorded simultaneously. The measured values of energy loss have been compared with the calculated values based on LSS theory [1], Northcliffe & Schilling [2], Ziegler et al. (ARIM-2003.20 code) [3], Hubert et al. [4] and Paul & Schinner [5] formulations. The experimentally measured straggling values have been compared with the corresponding calculated values using Bohr [6], Lindhard & Scharff [7], Bethe-Livingston [8] formulations. Merits and demerits of these formulations are highlighted. Some new interesting trends are observed.

It has been observed that the energy loss straggling increases almost linearly with the increase of energy loss irrespective of the nature of incident ion. The another interesting observation is that the energy loss straggling values for a particular ion in different polymers having almost same effective Z but with different chemical bonding, lie on the same curve, which authenticate the validity of Bragg's additivity rule.

REFERENCES

- [1] J. Lindhard, M. Scharff, H.E. Schiott, *Mat. Fys. Medd. Dan. Vid. Sels.* 33 (1963) 14.
- [2] L.C. Northcliffe, R.F. Schilling, *Nucl. Data Tables A7* (1970) 233.
- [3] J.F. Ziegler, J.P. Biersack, U. Littmark, in: *The stopping and Range of Ions in Solids, Vol.1*, Pergamon, New York, 1985.
- [4] F. Hubert, R. Bimbot, H. Gauvin, *At. Data Nucl. Data Tables* 46 (1) (1960).
- [5] H. Paul, A. Schinner, *Nucl. Instr. And Meth. B195* (2002) 166.
- [6] B. Bohr, *Mat. Fys. Medd. Dan. Vid. Selsk.* 18 (1948) 8.
- [7] J. Lindhard, M. Scharff, *Mat. Fys. Medd. Dan. Vid. Selsk.* 27 (1953) 15.
- [8] M.S. Livingston, H.A. Bethe, *Rev. Mod. Phys.* 9(1937) 245.

5.2.24 High Energy Ion-Irradiation Effects on Absorbed Water Relaxations in Kapton-H Polyimide

J.K. Quamara¹, Y. Sridharbabu¹, Randhir Singh¹, M.Garg¹, T. Prabha¹, Anu Sharma¹ and Fouran Singh²

¹Department of Applied Physics, National Institute of Technology, Kurukshetra-136119

²Nuclear Science Centre, New Delhi-110067

Water absorption relaxation (γ -relaxation) Process in kapton-H polyimide has been studied by many groups¹⁻³. Owing to its application as humidity sensors. The enhancement in this relaxation process due to high energy ion irradiation has been observed by the authors⁴. The present report deals with the detailed study of high energy ion irradiation effects (75 MeV Oxygen ion Fluences 1.8×10^{11} and $\times 10^{13}$ ions/cm²) on γ -relaxation process using field induced thermally stimulated current (FITSC) technique. Since this relaxation process mainly occur in the low temperature region (10⁰ to 40⁰C), we have confined our thermal spectrum between 10⁰ to 50⁰C. FITSC technique consist of two thermally activ-

ated processes namely thermally stimulated depolarization (TSD) thermally stimulated polarization (TSP) currents.

Fig (1) illustrates the representative TSDC characteristics of kapton-H polyimide (Poling Temperature $T_p=70^{\circ}\text{C}$, Poling Field $E_p=300\text{V}$) in the temperature range 10° to 50°C . Both pristine and irradiated samples were initially given a heat treatment to remove the spurious charges. The irradiated sample shows a very sharp maximum around 24°C .

In pristine sample also the evidence of this maximum is there but currents are much smaller as compared to that in irradiated samples. To know more about this relaxation, the TSPC current characteristics at various polarizing fields (E_p) have been obtained and shown in Fig (2). The low field TSPC characteristics clearly indicate a relaxation process in the form of current maximum. The absence of this current maximum at higher polarizing field may be due to the dominance of high temperature relaxation processes over the γ -relaxation.

The γ -relaxation which is mainly a water dependent relaxation process is quite complex and results from several competitive mechanisms involving various physical states of the absorbed water. The four carbonyl groups and the oxygen of the ether linkage in the structure of kapton-H polyimide are the most probable sites where the water molecule can be bound.

In Fig (3), the dielectric loss factor vs. temperature curve also indicates the presence of this relaxation process in the temperature region in the form of loss peaks. The presence of more than one loss peaks in this temperature region indicates the absorption of water in kapton-H polyimide taking place at different sites.

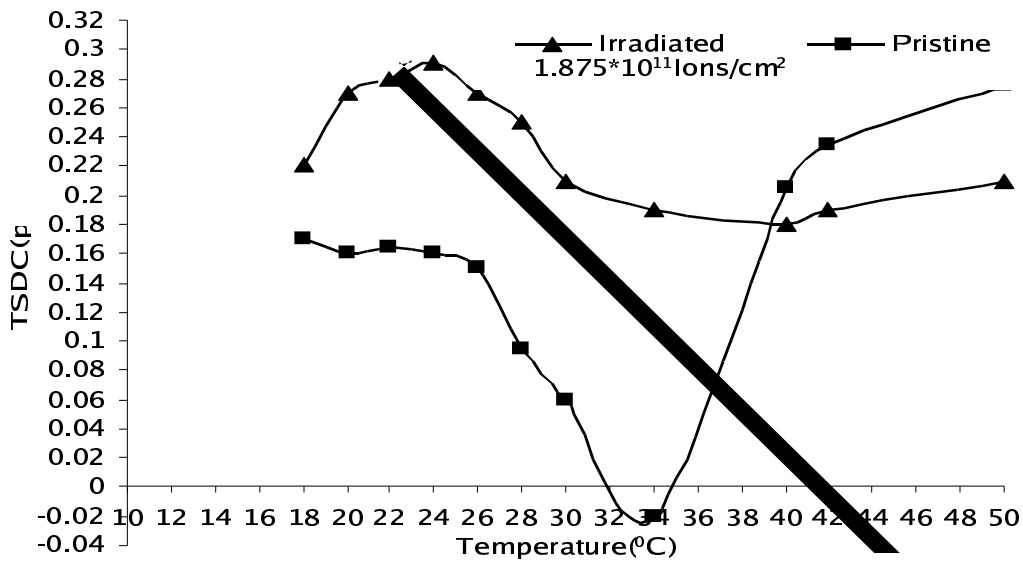


Fig.1: TSDC Spectrum for Irradiated and Pristine kapton-H samples

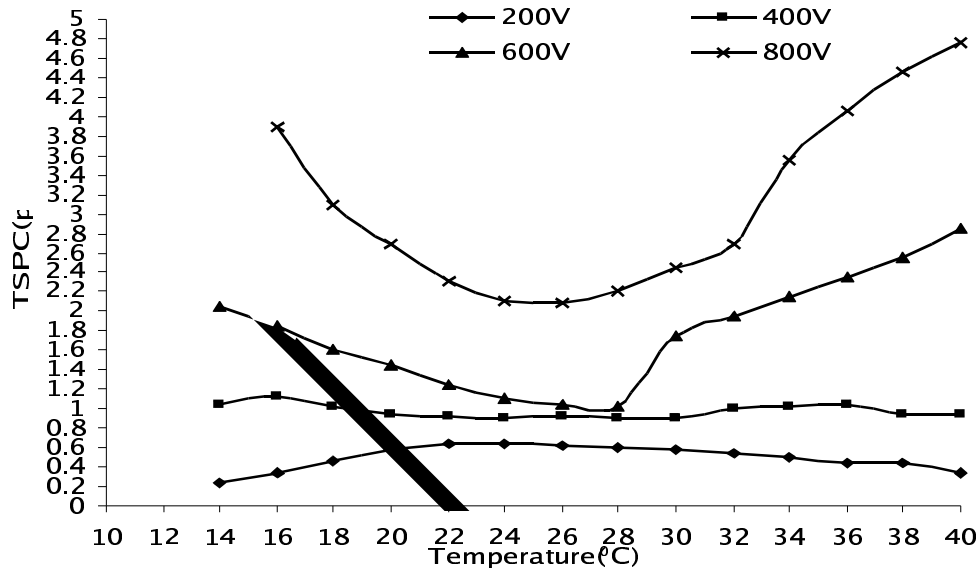


Fig. 2: TSPC Spectrum for Irradiated sample of kapton-H polyimide at different polarizing fields (Ep)

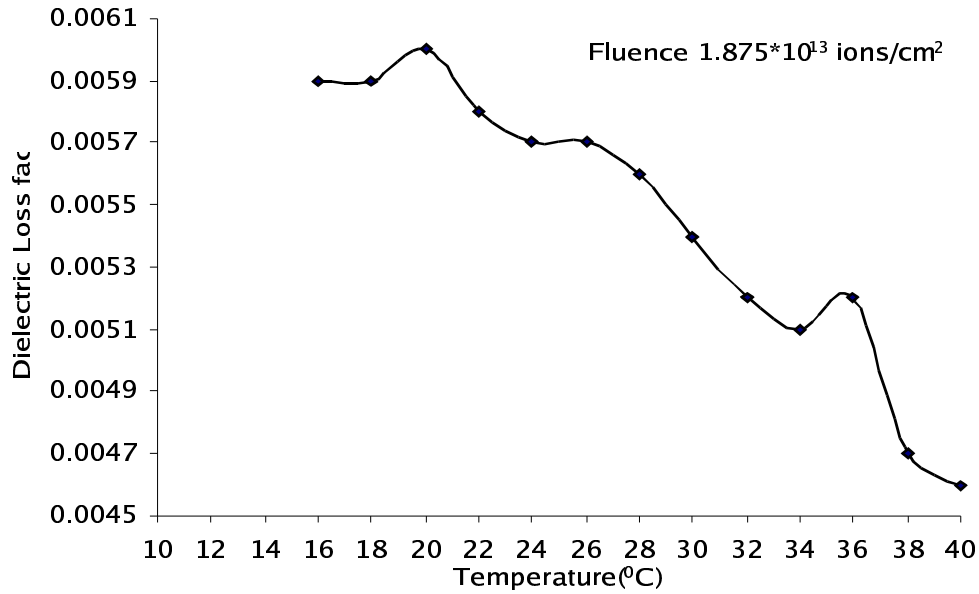


Fig. 3: Dielectric loss Factor vs. temperature in Irradiated kapton-H polyimide

REFERENCES

- [1] Melcher J, Yang Daben, Arlt G, *IEEE Transactions on Electrical Insulation*, 24-1 (1989) 31.
- [2] Shirnet V, Chaturvedi U K, Agrawal S K, in: Mittal K L, *Polyimide* (Ed.), Vol-1, Plenum Press, New York (1982) p. 555.
- [3] Chen C Ku, Liepins Raimond, *Electrical Properties of Polymers: Chemical Principles*, Hanser Publishers, New York (1987) p.20.

[4] Garg M., Quamara J K, *Nucl. Instr. and Meth. in Phys. Res. B*179 (2001) 83.

5.2.25 Investigations on the effect of SHI on the optical, electrical and structural properties of plasma polymerised organic thin films

S. Saravanan¹, M. R. Anantharaman¹, S. Venkatachalam², F. Singh³ and D. K. Avasthi³

¹Dept. of Physics, Cochin University of Science & Technology, Cochin - 682 022

²PSCD, Vikram Sarabhai Space Centre, Trivandrum - 695 022

³Nuclear Science Centre, New Delhi - 110 067

Modification of polymer thin films by swift heavy ions can induce irreversible changes in their structural, electrical and optical properties [1-3]. Polyaniline and polyfurfural thin films prepared by RF plasma polymerization were irradiated with 92 MeV Si ions for various fluences of 1×10^{11} ions/cm², 1×10^{12} ions/cm² and 1×10^{13} ions/cm². FTIR and UV-Vis NIR measurements were carried out on the pristine and silicon ion irradiated polyaniline/polyfurfural thin films for structural evaluation and optical bandgap determination. The photoluminescence studies on the pristine and irradiated samples of polyaniline and polyfurfural are also carried out.

Polyaniline and polyfurfural thin films of different thickness were prepared by RF plasma polymerisation. UV-Vis absorption studies and photoluminescence studies were carried out on these pristine and the irradiated polyaniline samples.

The FTIR spectra of polyaniline and polyfurfural were carried out. The band assignments of the FTIR spectrum of polyaniline pristine and irradiated are given in Table 1.

Table 1

FTIR assignments of Polyaniline Pristine and irradiated polyaniline at different fluences

Assignment	RF Polyaniline		
	Pristine	Irradiated	
		1×10^{11} ions/cm ²	1×10^{13} ions/cm ²
N-H Vibration	3207	3353	3340
C-H Stretch	2883	3058	3058
C-H Stretch	2834	2875	2873
$C \equiv C$	-	2132	2183
Ring Stretch	1656	1664	1565
Ring Stretch	1423	1436	1548
Ring Stretch			1444
CH in plane deformation	1059	1037	

C-N Stretch	971	973	975
C-N Stretch			1326
CH Out of plane deformation	783	804	825

The absorbance is plotted against the photon energy for polyaniline pristine and the irradiated polyaniline thin films. A satisfactory fit is obtained for $n=1/2$ showing the existence of direct allowed band gap. The intercept of this plot on the photon energy axis gives the bandgap of the samples. The bandgap decreases with increase of ion fluence. It can be seen that while pristine polyaniline exhibits a band gap 3.94 eV and polyaniline irradiated with fluence of 1×10^{13} ions/cm² has a band gap of 3.60 eV. During irradiation, the polymeric materials loose gas atoms and the enrichment of carbon atoms leads to the formation of hydrogenated amorphous carbon with optical energy gap depending on the H/C atom ratio. The swift heavy ions results in rearrangement and bond shifting which leads to ring opening in which $C \equiv C$ terminals are formed. In this process, the resulting product having more extended conjugated structure causing the decrease in band gap. The number of clusters are also estimated from the optical bandgap for both polyaniline and polyfurfural.

The dielectric permittivity of both pure and irradiated polyaniline and polyfurfural were carried out by employing a HP 4285A impedance analyser in the frequency range 100Hz – 1MHz. It has been found that both polyaniline and polyfurfural exhibit low k characteristics and irradiation induces structural changes and there by decreases the dielectric permittivity with irradiation.

Photoluminescence spectra were recorded for plasma polymerised aniline and furfural. The pristine sample exhibits the peaks at 575 nm and 680 nm. After irradiation the nature of PL spectrum remains similar but the peak intensity varied with the ion fluence.

In general the effect of irradiation can be viewed in two ways.

- 11 The restructuring of the surface chemical species because of the energy deposited through electronic loss during the process of irradiation
- 12 Formation of radiation induced defects leading to non-radiative recombination centres.

FTIR spectra indicate that the pristine polyaniline retains the benzene ring and the ring is not opened up. But after irradiation, the ring is opened up because of high-energy ions, which induce structural changes. The increase of intensity of a shoulder peak may be attributed to the rearrangement of bonds as well as the increase of conjugation in the polymer. The incident peak intensity decreases with ion fluence. This could be due to opening of benzene rings. This is in conformity with FTIR results. The change in optical band gaps for irradiated samples are evaluated and it is found that the optical band gap reduces with increase of fluence for both polyaniline and polyfurfural. The dielectric permittivity of both polyaniline and polyfurfural lie in the low k regime.

REFERENCES

- [1] C. Joseph Mathai, S. Saravanan, M. R. Anantharaman, S. Venkatachalam, S. Jayalekshmi: J. Phys. D: Appl. Phys. **35**, 240 (2002)
- [2] C. Joseph Mathai, S. Saravanan, M. R. Anantharaman, S. Venkatachalam, S. Jayalekshmi: J. Phys. D: Appl. Phys. **35**, 2206 (2002)
- [3] Effect of Swift Heavy Ions on the Structural and Optical Properties of RF Plasma Polymerized Aniline Thin Films S Saravanan, C Joseph Mathai, D K Avasthi, S Venkatachalam, M R Anantharaman AVS 50th International Symposium held at Baltimore, MD, USA during Nov. 2 - 7, 2003.

5.2.26 Correlation between Ion Track Diameter and Charge State of Incident Ion

DP Gupta¹, RS Chauhan², Shyam Kumar³, PK Diwan³, VK Mittal⁴, S. A. Khan⁵, Ambuj Tripathi⁵, Fouran Singh⁵, Santanu Ghosh⁵ and DK Avasthi⁵

¹Department of Applied Sciences, Chitkara Institute of Engineering and Technology, Rajpura – 140 401, Punjab,

²Department of Physics, RBS College, Agra

³Department of Physics, Kurukshetra University, Kurukshetra

⁴Department of Physics, Punjabi University, Patiala 147002

⁵Nuclear Science Centre, New Delhi-110067

When swift heavy ions are bombarded on non-conducting materials like polymers, part of the ion energy gets converted into atomic motion causing ejection of various species from the material. As a consequence, an ion track (a nanometric size cylindrical amorphized zone) is generated corresponding to each incident ion. It has been shown [1] by us that by measuring hydrogen evolved from a polymer under heavy ion bombardment, we can deduce the diameter of damaged zone or ion tracks formed in the polymer. It has been reported in literature [2-4] that hydrogen release from sample under heavy ion bombardment depends strongly upon the charge state of incident ion. In the present work, it was decided to measure the hydrogen evolved under heavy ion bombardment of polymers and to measure the radii of damaged zones or so called ion tracks formed in polymers as a function of charge state of the incident ion and hence to get information on ion-polymer interaction.

Ion beams of 130 MeV ¹⁰⁷Ag of charge states 11⁺, 14⁺ and 25⁺ were bombarded on Polystyrene (PS), Polypropylene (PP) and Polyethylene Terephthalate (PET). The polymer foils used in the present experiment had thicknesses between 6 to 20 micron. The loss of hydrogen as a function of ion fluence for different charge states for PP, PS and PET were fitted using two equations in two different regimes [1].

It is observed that the hydrogen released as well as track diameter depend strongly on the charge state of the incident ion. This behavior confirms the finding of Schiwietz and Grande that the electronic stopping power depends upon the charge state of the incident ion. The hydrogen loss curves were fitted with an equation of the type $y = \alpha q^n$ where

q is the charge on the incident ion and the value of the exponent n was found to vary between 1.4 to 2.0 contrary to earlier reported value of 2.7.

As is evident from table 1, radius of ion tracks formed in polymers depends upon the charge state of incident ion. Approximately when the charge state is doubled (from 11 to 25) radius of ion tracks increases by a factor of 2. Finally the ion track radii were fitted with an equation of the type $r = \beta q^m$, where q is again the charge of incident ion and the exponent m was found to vary between 0.63 to 0.88.

Table 1 : Total hydrogen released per incident ion for different charge state of ^{107}Ag ions on PP, PS and PET.

4th column of this Table shows the fitted equation $y = \alpha q^n$ for hydrogen released/ ion and 6th column shows similar fitted equation $r = \beta q^m$ for track radius

Polymer	Charge State	Hydrogen released/ ion (y) $\times 10^6$	$y = \alpha q^n$	Track radius r (nm)	$r = \beta q^m$
PP	11 ⁺	0.532	$\alpha = 2.20 \times 10^4$ $n = 1.414$	2.79	$\beta = 6.62 \times 10^{-10}$ $m = 0.63$
	14 ⁺	1.229		3.93	
	25 ⁺	1.916		4.91	
PS	11 ⁺	0.397	$\alpha = 5.09 \times 10^3$ $n = 1.832$	2.82	$\beta = 4.37 \times 10^{-10}$ $m = 0.79$
	14 ⁺	0.675		3.64	
	25 ⁺	1.825		5.48	
PET	11 ⁺	0.099	$\alpha = 7.69 \times 10^2$ $n = 2.06$	1.84	$\beta = 2.36 \times 10^{-10}$ $m = 0.88$
	14 ⁺	0.196		2.52	
	25 ⁺	0.560		3.88	

REFERENCES

- [1] V.K. Mittal, S. Lotha and D.K. Avasthi, Radiation Effects and Defects in Solids 147(1999) 199
- [2] S. Della Negra et al. IPN Annual Report 1990 p 138
- [3] A. Brunelle, S. Della-Negra, J. Depauw, H. Joret, Y. Le Beyec and K. Wien, Nucl. Instrum. and Methods B43(1989)484.
- [4] C.A. Brunelle et al, Nucl. Instrum Methods 43 (1983) 586.

5.2.27 Heavy Ion RBS with 12 MeV Carbon

S. A. Khan³, S. Kumar¹, M. Kumar², V. Baranwal², D. Agrawal¹, A. Tripathi³
and D. K. Awasthi³

¹Department of Physics, R. B. S. College, Agra-282 002

²Department of Physics, University of Allahabad, Allahabad-211 002

³Nuclear Science Centre, New Delhi-110 067

The experiment conducted to check the feasibility of doing HIRBS at Nuclear Science Centre with 12 MeV C is reported here. The beam energy could not be lowered due to technical constraints. Lower energy would have increased the cross-section. GPSC beam line was used in the experiment that has the scattering chamber of diameter of 1.5 m.

The sample was placed at an angle of 45° from the direction of the incident ion beam. The SSBD detector (active area: 100 mm², depletion depth: 500 micron) was fixed at right angle to the beam direction. This geometry was chosen to enhance the depth resolution and scattering cross-section. A slit of 38 mm² area was fixed in front of the detector to avoid edge effect. The detector subtended a solid angle of 2.9 msr.

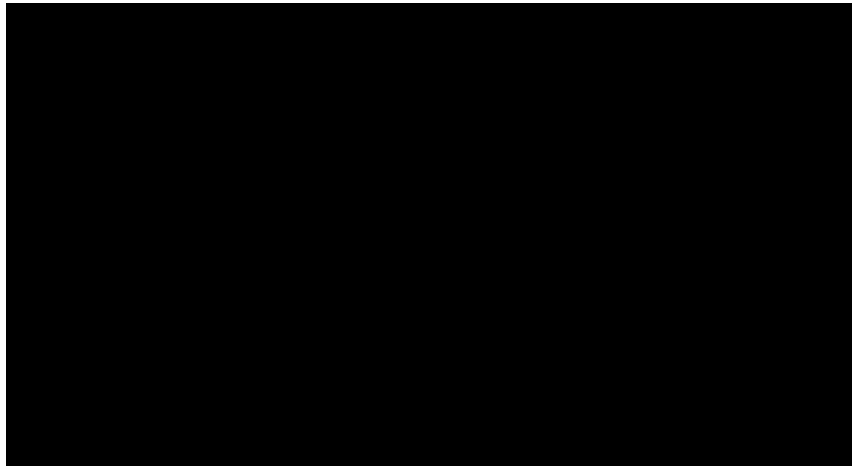


Fig. 1: HIRBS spectrum of Si(100)/Cu/Ge/Al sample

The HIRBS spectrum of the sample, having Al (20 nm), Ge (65 nm) and Cu (60 nm) layers on Si (100) substrate is shown in Figure 1. These samples were prepared for studies of ion beam induced mixing across the interfaces. Energy resolution of the system is 80 keV for 10.6 MeV backscattered carbon. The corresponding depth resolution can be quoted as 10 nm for near surface region. Even though energy resolution is poor in case of HIRBS, the depth resolution is nearly the same as conventional RBS with He because of chosen geometry and higher stopping power of carbon.

5.2.28 Heavy ion testing of VLSI devices for Single Event Effects

S.B. Umesh¹, G.R.Joshi¹, Sandhya Raghunath¹ and S.R. Kulkarni²

¹ISRO Satellite Centre, Vimanapura post, Air Port Road, Bangalore –560 017

²Department of Physics, Bangalore University, Bangalore-560 056

The space environment of LEO and GEO contains high energy particulate radiation in the energy levels of a few MeV to hundreds of MeV. The sub micron CMOS VLSI devices in particular, are very sensitive to particulate radiation as compared to other technology devices. The high energy particles impinging on these devices can cause SEU and SEL, resulting in device degradation or total failure. Spacecraft systems use radiation hardened hi-rel integrated circuits to protect against Total Ionization Dose (TID) effects and Single Event Effects (SEE) such as Single Event Upset (SEU) and Single Event Latch up (SEL). Radhard ICs have protection against both TID & SEE effects.

In case of non-availability of radhard ICs, rad tolerant devices are chosen after examining the criticality of the device application. 128k x 8 SRAM and 4k x 9 FIFO from M/s. Atmel are rad tolerant devices. To characterize these devices for LET thresholds, heavy ion radiation testing was conducted at Nuclear Science Centre, New Delhi. In addition to these devices, an 883 level 1MB EEPROM from M/s Atmel used in launch vehicle programme, a radhard MIL – STD – 1553B Bus controller IC from M/s DDC and Bulk CMOS shift register IC from M/s Intersil and M/s STM were also tested for SEE effects. The devices were first exposed to low flux of heavy ions Silicon (Si⁺) and then Silver (Ag⁺). Besides these devices, diode 1N5811, which is proposed to be mounted outside the spacecraft and would thus be subjected to heavy ion irradiation was also tested for SEE effects.

Device Types Tested and Testing Methodologies

(a) SRAM 65608E , FIFO 67204F, EEPROM AT28C010

All locations of 128k x 8 SRAM, 4k x 9 FIFO, 128k x 8 EEPROM are filled with checkerboard pattern of 55_h(01010101) & AA_h(10101010) in alternate locations during irradiation. Data stored in the memory is continuously read and verified with the reference data pattern. In the event of any upset, the failure is recorded and the data is re-written again. This reading and writing process continues during the whole of exposure duration.

(b) SHIFT REGISTER 4094B

The 8-bit store and shift register is stored with a data pattern of alternate 1's & 0's and the data stored in the shift register continuously verified with the initially stored pattern and any data upset is recorded and monitored.

(c) **MIL – STD – 1553 BC/RT 61582**

The device 61582 operates in either Bus Controller (BC) or Remote Terminal (RT) mode of operation and has two bi-directional serial interface buses A & B for transmission & reception of data in the Manchester coded data format.

The test system checks the DUT in the BC/RT mode of operation for transmission & reception of data with another device acting as RT/BC for both bus A & B. The system also checks the device’s internal 16k × 16 SRAM for the checkerboard pattern of 5555_h & AAAA_h. Any upsets in the internal RAM or in the transmission/reception control word/data are recorded and monitored during irradiation.

Table 1

S.No	Device type	ion	Energy MeV	LET MeV -cm ² /mg	Flux P /cm ² /s	Fluence P/cm ²	SEU	SEL
1.	65608E	²⁸ Si ⁸⁺	100	11	300	2.7 X 10 ⁵	Upsets overflow	No Latch – up
		¹⁰⁷ Ag ⁸⁺	70	42	300	2.7 X 10 ⁵	Upsets overflow	No Latch – up
2.	67204F	²⁸ Si ⁸⁺	100	11	300	2.7 X 10 ⁵	~ 9000 up-sets/hour	No Latch – up
3.	AT28C010	²⁸ Si ⁸⁺	100	11	300	5.4 X 10 ⁵	No upsets	No Latch – up
		¹⁰⁷ Ag ⁸⁺	70	42	300	5.4 X 10 ⁵	No upsets	No Latch – up
4.	BU61582	²⁸ Si ⁸⁺	100	11	300	5.4 X 10 ⁵	No upsets	No Latch – up
5.	1N5811	²⁸ Si ⁸⁺	100	11	300	2.16X 10 ⁶	-	-
		¹⁰⁷ Ag ⁸⁺	70	42	300	2.16X 10 ⁶	-	-
6	4094B	¹⁰⁷ Ag ⁸⁺	70	42	300	5.4 X 10 ⁵	No upsets	No Latch – up

Table shows the test results of SEU and SEL of all the devices exposed to heavy ion irradiation.

The following observations were made based on above investigations:

- 13 The Atmel rad tolerant devices 128K × 8 SRAM 65608E & 4k × 9 FIFO 67204F as **expected are found to be very sensitive to particulate radiation.**
- 14 The 128K x 8 EEPROM AT28C010 is a Mil – Std – 883 level, non-radiation hardened device. Further tests are required to be conducted with more samples to

confirm the test results.

- 15 The shift register IC 4094B was exposed to both $^{28}\text{Si}^{8+}$ and $^{107}\text{Ag}^8$ and passed. This shows that the device LET_{th} for SEU & SEL is beyond 42 MeV-cm²/mg.
- 16 The DDC make radiation hardened Mil – Std – 1553B BC/RT 61582 was tested to heavy ion irradiation as a part of verification of the manufacturers test data. No SEU or SEL was observed and the device functioned normally.
- 17 The diode 1N5811 was exposed to both $^{28}\text{Si}^{8+}$ and $^{107}\text{Ag}^8$ and did not show any failure.